Omenn syndrome in a patient with RAG1-deficient severe combined immunodeficiency. Blood. 2005;106:2099–101.
24. Ariga T, Kondoh T, Yamaguchi K, et al. Spontaneous in vivo reversion of an inherited mutation in the Wiskott–Aldrich syndrome. J Immunol. 2001;166:5245–9.
25. Filipe-Santos O, Bustamante J, Haverkamp MH, et al. X-linked susceptibility to mycobacteria is caused by mutations in NEMO impairing CD40-dependent IL-12 production. J Exp Med. 2006;203:1745–59.
26. Nenci A, Huth M, Funteh A, et al. Skin lesion development in a mouse model of incontinentia pigmenti is triggered by NEMO deficiency in epidermal keratinocytes and requires TNF signaling. Hum Mol Genet. 2006;15:531–42.
27. Van den Brande J, Braat H, van den Brink G, et al. Infliximab but not etanercept induces apoptosis in lamina propria T-lymphocytes from patients with Crohn's disease. Gastroenterology. 2003;124:1774–85.
28. Nos P, Bastida G, Beltran B, et al. Crohn's disease in common variable immunodeficiency: treatment with antitumor necrosis factor alpha. Am J Gastroenterol. 2006;101:2165–6.
29. Chua I, Standish R, Lear S, et al. Anti-tumour necrosis factor-alpha therapy for severe enteropathy in patients with common variable immunodeficiency (CVID). Clin Exp Immunol. 2007;150:306–11.
30. Uzel G, Orange JS, Poliak N, et al. Complications of tumor necrosis factor-α blockade in chronic granulomatous disease-related colitis. Clin Infect Dis. 2010;51:1429–34.
31. Mackey AC, Green L, Liang LC, et al. Hepatosplenic T cell lymphoma associated with infliximab use in young patients treated for inflammatory bowel disease. J Pediatr Gastroenterol Nutr. 2007;44:265–7.
32. Mackey AC, Green L, Leptak C, et al. Hepatosplenic T cell lymphoma associated with infliximab use in young patients treated for inflammatory bowel disease: update. J Pediatr Gastroenterol Nutr. 2009;48:386–8.
33. Diak P, Siegel J, La Grenade L, et al. Tumor necrosis factor alpha blockers and malignancy in children: forty-eight cases reported to the Food and Drug Administration. Arthritis Rheum. 2010;62:2517–24.

Chronic Mucocutaneous Candidiasis Caused by a Gain-of-Function Mutation in the STAT1 DNA-Binding Domain

Shunichiro Takezaki,*,[1] Masafumi Yamada,*,[1] Masahiko Kato,† Myoung-ja Park,‡ Kenichi Maruyama,§ Yasuhiro Yamazaki,* Natsuko Chida,*,¶ Osamu Ohara,‖ Ichiro Kobayashi,* and Tadashi Ariga*

Chronic mucocutaneous candidiasis (CMC) is a heterogeneous group of primary immunodeficiency diseases characterized by chronic and recurrent *Candida* infections of the skin, nails, and oropharynx. Gain-of-function mutations in *STAT1* were very recently shown to be responsible for autosomal-dominant or sporadic cases of CMC. The reported mutations have been exclusively localized in the coiled-coil domain, resulting in impaired dephosphorylation of STAT1. However, recent crystallographic analysis and direct mutagenesis experiments indicate that mutations affecting the DNA-binding domain of STAT1 could also lead to persistent phosphorylation of STAT1. To our knowledge, this study shows for the first time that a DNA-binding domain mutation of c.1153C>T in exon 14 (p.T385M) is the genetic cause of sporadic CMC in two unrelated Japanese patients. The underlying mechanisms involve a gain of STAT1 function due to impaired dephosphorylation as observed in the coiled-coil domain mutations. ***The Journal of Immunology*****, 2012, 189: 1521–1526.**

Chronic mucocutaneous candidiasis (CMC) is a heterogeneous group of primary immunodeficiency diseases characterized by chronic and recurrent *Candida* infections of the skin, nails, and oropharynx (1). It is often associated with a variety of endocrine or autoimmune disorders. Especially, in autoimmune polyendocrinopathy with candidiasis and ectodermal dystrophy, mucocutaneous candidiasis is accompanied by hypoparathyroidism, adrenal failure, insulin-dependent diabetes mellitus, alopecia, and malabsorption syndrome (2). Although autosomal-dominant forms of CMC are also associated with endocrine disorders, such as hypothyroidism (3), the genetic causes of these disorders had remained unknown until very recently.

In 2011, two groups reported that autosomal-dominant CMC and sporadic CMC are caused by mutations in *STAT1* (4–6). The reported mutations have been exclusively localized in the coiled-coil (CC) domain, leading to gain of STAT1 function due to impaired STAT1 dephosphorylation (4). However, crystallographic analysis and direct mutagenesis experiments indicated that mutations in the DNA-binding domain (DBD) could also cause a resistance to dephosphorylation (7, 8). To our knowledge, this is the first study to demonstrate that a mutation affecting the DBD of STAT1 is the genetic cause of sporadic CMC in two unrelated Japanese patients. The mechanisms involve a gain of STAT1 function due to impaired dephosphorylation of STAT1, as also observed in mutations affecting the CC domain.

Materials and Methods

Patients

Patient 1 is a 12-y-old boy born to nonconsanguineous healthy Japanese parents. He developed severe and recurrent oral thrush since the age of 2 y and was diagnosed with CMC. He has also had recurrent pneumonia, bronchitis, and otitis media caused by *Streptococcus pneumoniae* since the age of 3 y. Chest x-ray and computerized tomography scan demonstrated the presence of bronchiectasis at the age of 5 y. He was noticed to have hypothyroidism with positive anti–thyroid-stimulating hormone receptor Abs, and levothyroxine was initiated at the age of 9 y.

Patient 2 is a boy born to nonconsanguineous healthy Japanese parents. He had poor body weight gain soon after birth. He was diagnosed with CMC at the age of 6 y. He also had recurrent bronchitis, pneumonia, and sinusitis caused by *S. pneumoniae*. He was diagnosed with bronchiectasis at the age of 7 y. At the age of 13 y, he developed hemophagocytic lymphohistiocytosis (HLH). He subsequently presented with autoimmune hemolytic anemia with positive direct and indirect Coombs' tests and thrombocytopenia and was diagnosed as having Evans syndrome. He died suddenly at the age of 14 y and 5 mo from disseminated intravascular coagulation and pulmonary insufficiency of unknown etiology. These two patients were not related (case reports in preparation).

Patient 3 is a 15-y-old girl with CMC. Her father had also been diagnosed with CMC and died of cerebral vasculitis (9). She was demonstrated to have the heterozygous R274Q mutation affecting the CC domain of STAT1. Because this mutation was recently reported as a gain-of-function mutation due to impaired dephosphorylation of STAT1 (4), we studied Patient 3 as a control for investigating the mechanisms of the development of CMC in Patients 1 and 2. Informed consent for genetic analysis was obtained from the patients, their family members, and normal controls under a protocol approved by the Institutional Review Board of Hokkaido University Hospital.

*Department of Pediatrics, Hokkaido University Graduate School of Medicine, Sapporo 060-8638, Japan; †Department of Allergy and Immunology, Gunma Children's Medical Center, Shibukawa 377-8577, Japan; ‡Department of Hematology/Oncology, Gunma Children's Medical Center, Shibukawa 377-8577, Japan; §Department of Nephrology, Gunma Children's Medical Center, 377-8577, Shibukawa, Japan; ¶Department of Dentistry for Children and Disabled Persons, Hokkaido University Graduate School of Dental Medicine, Sapporo 060-8586, Japan; and ‖Department of Human Genome Technology, Kazusa DNA Research Institute, Chiba 292-0818, Japan

[1]S.T. and M.Y. contributed equally to this work.

Received for publication March 28, 2012. Accepted for publication May 25, 2012.

This work was supported in part by a grant for Research on Intractable Diseases from the Japanese Ministry of Health, Labor and Welfare and a grant from the Hokkaido University Frontier Foundation.

Address correspondence and reprint requests to Dr. Masafumi Yamada, Department of Pediatrics, Hokkaido University Graduate School of Medicine, North 15 West 7, Kita-ku, Sapporo 060-8638, Japan. E-mail address: yamadam@med.hokudai.ac.jp

Abbreviations used in this article: CC, coiled-coil; CMC, chronic mucocutaneous candidiasis; DBD, DNA-binding domain; HLH, hemophagocytic lymphohistiocytosis; STAT1p, phosphorylated STAT1; Wt, wild-type.

www.jimmunol.org/cgi/doi/10.4049/jimmunol.1200926

Generation of EBV-transformed cell lines

EBV-transformed cell lines (EBV-LCLs) were generated by in vitro transformation of human B cells with EBV (strain B95-8), as described elsewhere (10). Based on the results of *STAT1* sequence analysis, EBV-LCLs from Patient 1 with T385M and wild-type (Wt) alleles and Patient 3 with R274Q and Wt alleles were designated as T385M/Wt and R274Q/Wt, respectively. Two age-matched control EBV-LCLs, designated Wt-1 and Wt-2, were used as controls. EBV-LCLs from Patient 2 were not obtained.

Stimulation reagents

For stimulation, 1:1000 diluted recombinant human IFN-γ 1a (Shionogi, Osaka, Japan; 1000 JRU/ml, 200 ng/ml), 1500 U/ml recombinant human IFN-α (Biosource International, Camarillo, CA), 20 ng/ml IL-27 (R&D Systems, Minneapolis, MN), and 100 μg/ml Curdlan (Wako, Osaka, Japan) were used.

DNA isolation, PCR, and sequence analysis of PCR products and TOPO-TA clones

These procedures were performed following the methods described elsewhere (10).

Measurement of CXCL10 (IP-10) concentration in supernatant of monocyte-derived macrophages and EBV-LCLs using Cytometric Bead Array

To accurately evaluate STAT1 function by studying supernatant IP-10 production from macrophages, monocytes were first purified from PBMCs with CD14 MicroBeads (Miltenyi Biotec, Bergisch Gladbach, Germany) to avoid contamination of other cells. A total of 5×10^5 cells/ml monocytes was then differentiated into macrophages by culturing for 7 d in RPMI 1640 containing 10% FBS in the presence of 5 ng/ml M-CSF (R&D Systems). To determine the effect of IFN-γ, differentiated macrophages in triplicate were not stimulated, were stimulated with 1 μg/ml LPS (Sigma, St Louis, MO), or were prestimulated with 1000 U/ml (200 ng/ml) IFN-γ (Shionogi) for 2 h and then stimulated with 1 μg/ml LPS for 24 h (IFN-γ–LPS stimulation), and supernatant was harvested for IP-10 measurement. For studying IP-10 production from EBV-LCLs, 1×10^6 cells/ml EBV-LCLs were cultured in the presence of 1000 U/ml IFN-γ for 6 h. The concentration of IP-10 in the supernatant was measured with Cytometric Bead Array (BD, San Diego, CA), following the manufacturer's instructions. Data from triplicate independent experiments are reported as the mean ± SD.

Preparation of nuclear extract

Nuclear extract was prepared essentially as described previously (11). Briefly, harvested cells were washed with Ca^{2+} and Mg^{2+}-free PBS and pelleted by centrifugation at 1500 × *g* for 5 min at 4°C. The resulting cell pellets were resuspended in cytoplasmic extract buffer (10 mM HEPES [pH 7.9], 10 mM KCl, 0.1 mM EDTA, 0.1 mM EGTA, 1 mM DTT, 1 mM Na_3VO_4, 1 mM NaF [pH 8]) with the addition of the recommended volume of dissolved protease inhibitor mixture tablets (Roche). After incubation on ice for 15 min, a 1:16 volume of 10% Nonidet P-40 was added. The suspension was vortexed and then centrifuged at 1500 × *g* for 5 min at 4°C. The pellets were washed again with cytoplasmic extract buffer without Nonidet P-40, resuspended with nuclear extract buffer (20 mM HEPES [pH 7.9], 400 mM NaCl, 1 mM EDTA, 1 mM EGTA, 1 mM DTT, 1 mM Na_3VO_4, 1 mM NaF [pH 8]) with the addition of protease inhibitor, and incubated at 4°C for 30 min. After centrifugation at maximum speed for 5 min at 4°C, the supernatant was saved as nuclear extract. Protein concentration was measured by Protein Assay (Bio-Rad, Hercules, CA).

Western blot analysis

After addition of SDS sample buffer, 10 μg nuclear extract was separated by 7.5% polyacrylamide gels and transferred to Immobilon-P Transfer Membranes (Millipore, Billerica, MA). Anti-lamin A Ab (BioLegend, San Diego, CA) was used as a loading control for nuclear extract. All of the primary Abs were used at the final concentration of 1 μg/ml. HRP-conjugated anti-mouse IgG secondary Abs (GE Healthcare, Buckinghamshire, U.K.) were used at 1:2000 dilution. The blots were then visualized by Pierce Western blotting Substrate (Thermo, Rockford, IL).

Studies of STAT1 phosphorylation state and staurosporine and pervanadate treatment of cells

We assessed dephosphorylation with the tyrosine kinase inhibitor staurosporine in EBV-LCLs. A total of 1×10^6 cells/ml EBV-LCLs was stimulated with IFN-γ for 30 min and then incubated with 1 μM staurosporine (Alomone Labs, Jerusalem, Israel) for 15, 30, or 60 min. The phosphatase inhibitor pervanadate was prepared by mixing 200 mM sodium orthovanadate (Wako, Osaka, Japan) and 100 mM H_2O_2 at a 2:1 ratio for 15 min at 22°C. EBV-LCLs were treated with pervanadate (0.8 mM orthovanadate and 0.2 mM H_2O_2) for 5 min and then stimulated with IFN-γ for 30 min. The nuclear extract from each condition was subjected to SDS-PAGE. The phosphorylation state of STAT1 was evaluated with anti-human STAT1 (pY701) Ab purchased from BD. The membrane was then stripped and reprobed with anti-human STAT1 (BD) and anti-lamin A (BioLegend) Abs.

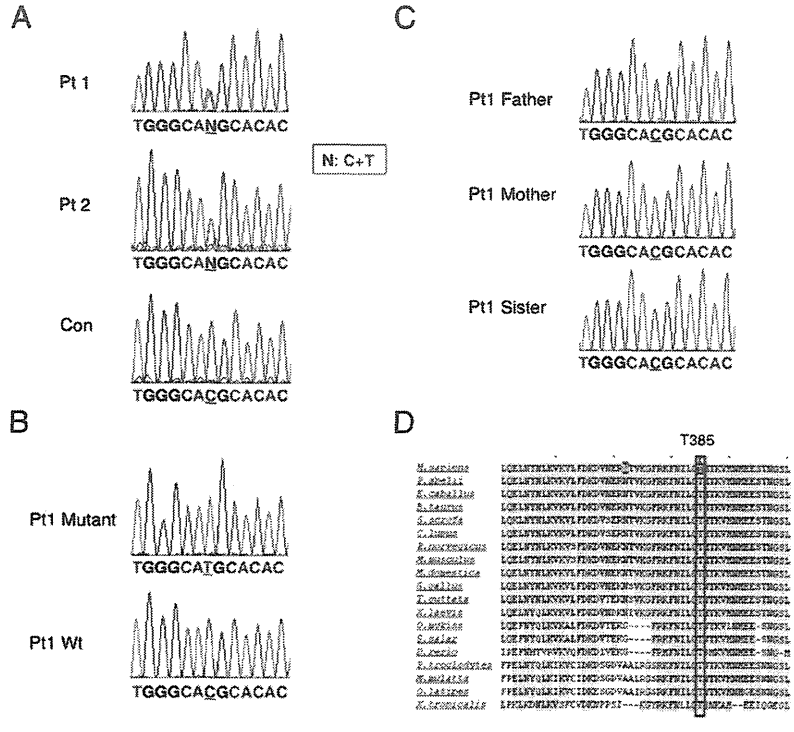

FIGURE 1. Patients 1 and 2 had the same heterozygous base change of c.1153C>T resulting in p.T385M in *STAT1*. (**A**) Direct sequence analysis of *STAT1* exon 14 in Patient 1 (Pt1) and Patient 2 (Pt2). Forward sequence is shown. (**B**) Sequence analysis of TOPO-TA clones of *STAT1* exon 14 PCR products in Patient 1. Mutant and Wt sequences are shown. (**C**) Direct sequence analysis of *STAT1* exon 14 in Patient 1's family members. (**D**) Comparison of the amino acid sequences of STAT1 in different species. The red box indicates the amino acids corresponding to p.T385 in humans. Con, Control.

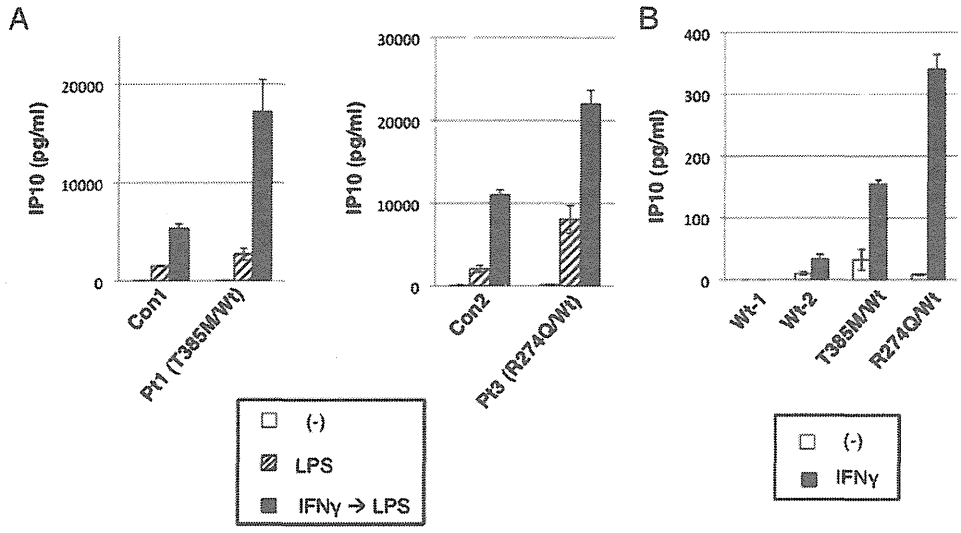

FIGURE 2. T385M was associated with higher levels of IP-10 production following IFN-γ stimulation in monocyte-derived macrophages and in EBV-LCLs. (**A**) Monocyte-derived macrophages were cultured in the presence of media, LPS, or IFN-γ–LPS for 24 h. IP-10 production was studied in the supernatant. Data shown are mean ± SD of triplicate independent experiments. (**B**) EBV-LCLs were stimulated with IFN-γ for 6 h, and IP-10 production was studied in the supernatant. Data shown are mean ± SD of triplicate independent experiments. Con1, Control for Patient 1 obtained and analyzed at the same time; Con2, control for Patient 3 obtained and analyzed at the same time; Pt1, Patient 1; Pt3, Patient 3; (−), media.

Flow cytometric analysis of intracellular IL-17A expression in CD4$^+$ cells

PBMCs at a density of 1 × 10^6 cells/ml were stimulated with 20 ng/ml PMA plus 500 ng/ml ionomycin for 6 h in the presence of GolgiStop (BD). Harvested PBMCs were washed and stained with PECy5-conjugated anti-human CD4 Ab (BioLegend) for 20 min at 4°C. Cells were washed three times and fixed and permeabilized with Cytofix/Cytoperm solution (BD) for 20 min at 4°C. Cells were then washed, incubated for 30 min with PE-conjugated anti-human IL-17A (BioLegend) or FITC-conjugated anti-human IFN-γ Abs (BioLegend), washed, and analyzed with a FACSCalibur (BD).

Results

A possible DBD mutation in STAT1

We first performed direct sequence analysis of the genes responsible for CMC in our patients: *AIRE*, *CLEC7A*, *CARD9*, *IL17RA*, *IL17F*, *IL2Rα*, and *STAT1* (4–6, 12–17). This study demonstrated that Patient 1 and Patient 2 have the same heterozygous base change in *STAT1* (c.1154C>T, p.T385M) (Fig. 1A), which was confirmed by the sequence analysis of TOPO-TA clones (Fig. 1B, data not shown). This base change has not been reported either as a mutation or as a single nucleotide polymorphism in the National Center for Biotechnology Information database, Ensembl database, or the Single Nucleotide Polymorphism Database, and it was not present in the family members of Patient 1 (Fig. 1C) or in 108 normal healthy controls (data not shown). Furthermore, the affected residue was evolutionarily conserved, as shown in Fig. 1D. The polymorphism phenotype-2 (PolyPhen-2) algorithm (http://genetics.bwh.harvard.edu/pph2/index.shtml), a structure sequence-based amino acid substitution-prediction method, predicted p.T385M as probably damaging, with a score of 1.000 (sensitivity: 0.00; specificity: 1.00). The sort intolerant from tolerant algorithm (http://sift.jcvi.org/) also predicted this amino acid substitution as deleterious. These results strongly indicate that c.1153C>T (p.T385M) is a de novo disease-causing mutation. Patient 1 was also shown to have an unreported heterozygous base change in *CARD9* (c.661G>A, p.K221E). However, this base change was also detected in his healthy father (data not shown). Additionally, PBMCs from Patient 1 showed normal IL-6 production in response

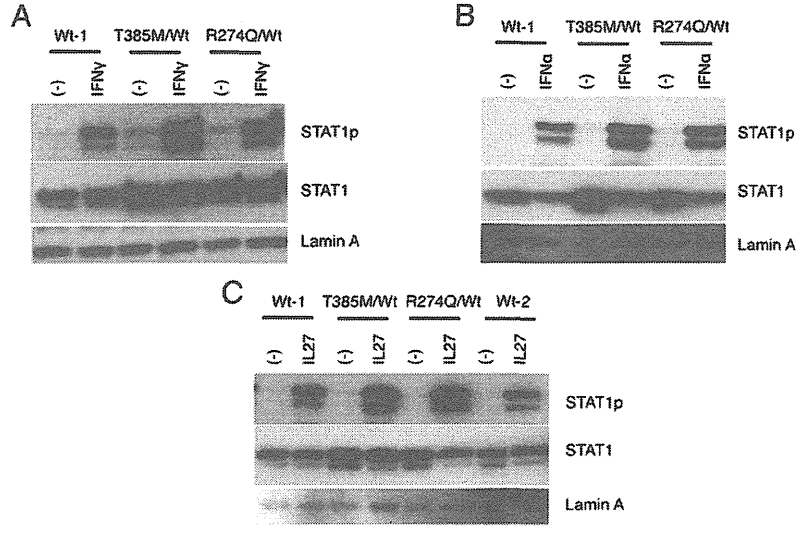

FIGURE 3. T385M was associated with hyperphosphorylation of STAT1 in response to IFN-γ, IFN-α, and IL-27 stimulation. Western blot analysis of STAT1p in nuclear extracts from EBV-LCLs was performed. Lamin A was used as a loading control. STAT1p expression in EBV-LCLs following IFN-γ (**A**), IFN-α (**B**), or IL-27 (**C**) stimulation for 30 min. (−), No stimulation.

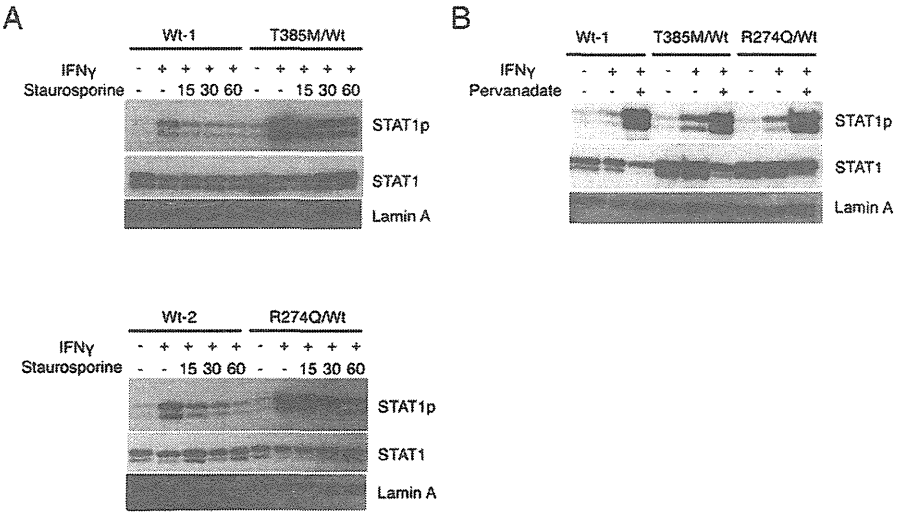

FIGURE 4. T385M was associated with hyperphosphorylation of STAT1 due to impaired dephosphorylation. (**A**) STAT1p expression in EBV-LCLs stimulated with IFN-γ for 30 min and then incubated with 1 μM staurosporine for 15, 30, or 60 min. (**B**) STAT1p expression in EBV-LCLs treated with pervanadate for 5 min and then stimulated with IFN-γ for 30 min.

to β-D-glucan stimulation with Curdlan (data not shown), indicating that the base change of c.661G>A, p.K221E in *CARD9* is not a disease-causing mutation but a single nucleotide polymorphism. The rest of the genes studied were demonstrated to be normal in both patients.

T385M is associated with gain of STAT1 function

Gain-of-function mutations in *STAT1* were very recently shown to be the genetic cause of autosomal-dominant or sporadic CMC (4–6). The reported mutations have been exclusively localized in the CC domain, leading to gain of STAT1 function due to impaired STAT1 dephosphorylation (4). To study whether the base change of c.1153C>T, p.T385M affecting the DBD of STAT1 also leads to gain of STAT1 function, the production of the downstream target of STAT1, IP-10, was studied following IFN-γ stimulation. IP-10 production was significantly higher in monocyte-derived macrophages from Patient 1 (T385M/Wt) and Patient 3 (R274Q/Wt) than in the matched control macrophages after IFN-γ–LPS stimulation (Fig. 2A). IP-10 production was also significantly higher in EBV-LCLs from Patient 1 (T385M/Wt) and Patient 3 (R274Q/Wt) after IFN-γ stimulation (Fig. 2B). These results indicated that T385M is a mutation leading to gain of STAT1 function.

STAT1 T385M leads to STAT1 hyperphosphorylation in response to IFN-γ, IFN-α, and IL-27 stimulation, which is due to impaired dephosphorylation

We then studied the STAT1 phosphorylation state in EBV-LCLs to determine the mechanisms of the gain of STAT1 function. Expression of phosphorylated STAT1 (STAT1p) protein following IFN-γ stimulation was higher in T385M/Wt and R274Q/Wt EBV-LCLs than in Wt EBV-LCLs (Fig. 3A). The hyperphosphorylated state of STAT1 was also observed following stimulation with IFN-α and IL-27 (Fig. 3B, 3C). Additionally, expression of total STAT1 in nuclear extract tends to be higher in T385M/Wt and R274Q/Wt EBV-LCLs than in Wt EBV-LCLs, especially without stimulation (Fig. 3). The mechanisms underlying STAT1 hyperphosphorylation in T385M/Wt EBV-LCLs were further explored with the tyrosine kinase inhibitor staurosporine and the phosphatase inhibitor pervanadate. The dephosphorylation of IFN-γ–ac-

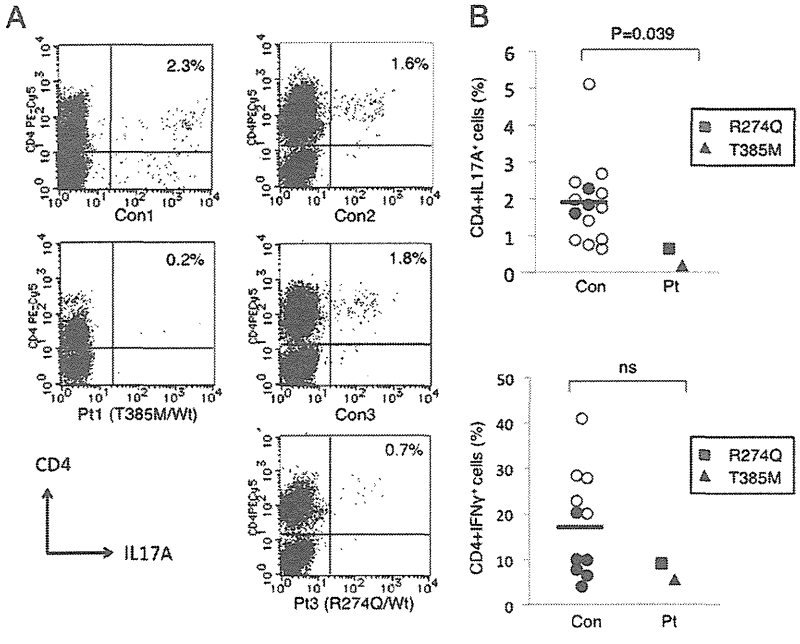

FIGURE 5. Patients 1 and 3 had deficient $CD4^+IL\text{-}17A^+$ cells but normal $CD4^+IFN\text{-}\gamma^+$ cells in response to PMA plus ionomycin stimulation. (**A**) Flow cytometric analysis of intracellular IL-17A expression following PMA plus ionomycin stimulation for 6 h. The proportion of $CD4^+IL\text{-}17A^+$ cells among $CD4^+$ cells was shown. (**B**) The proportion of $CD4^+IL\text{-}17A^+$ cells and $CD4^+IFN\text{-}\gamma^+$ cells among $CD4^+$ cells in normal controls and the patients. The horizontal lines indicate the mean proportion of $CD4^+IL\text{-}17A^+$ cells or $CD4^+IFN\text{-}\gamma^+$ cells in controls. Red and blue circles indicate controls obtained and analyzed at the same time as Patients 1 and 3, respectively. The *p* value was estimated using the Mann–Whitney *U* test. Con1, Control for Patient 1 obtained and analyzed at the same time; Con2 and Con3, controls for Patient 3 obtained and analyzed at the same time; Pt1, Patient 1; Pt3, Patient 3.

tivated T385M/Wt EBV-LCLs was impaired in the presence of staurosporine, as observed in R274Q/Wt EBV-LCLs (Fig. 4A). In contrast, with pervanadate treatment, the phosphorylation of STAT1 in T385M/Wt EBV-LCLs was similar to that seen in Wt EBV-LCLs (Fig. 4B). Therefore, the mechanisms underlying STAT1 hyperphosphorylation in T385M/Wt EBV-LCLs involve impaired dephosphorylation of STAT1, as observed in R274Q/Wt EBV-LCLs.

Patient 1 with the heterozygous T385M mutation in STAT1 had deficient Th17 cells

Deficient development of Th17 cells was documented to be associated with the development of CMC. CMC patients with gain-of-function mutations of *STAT1* affecting the CC domain have shown this defect (4). Therefore, we studied the proportion of $CD4^+IL\text{-}17A^+$ cells among $CD4^+$ cells in our patients after PMA plus ionomycin stimulation for 6 h. We also studied the population of $CD4^+IFN\text{-}\gamma^+$ cells to evaluate Th1 development. Patient 1 with the heterozygous T385M/Wt mutation of *STAT1* was reproducibly demonstrated to have dramatically reduced $CD4^+IL\text{-}17A^+$ cells (0.2% of $CD4^+$ cells), and Patient 3 with the heterozygous R274Q mutation had significantly reduced, but a little higher, $CD4^+IL\text{-}17A^+$ cells (0.7% of $CD4^+$ cells) (Fig. 5). The p value estimated using the Mann–Whitney U test was 0.039 between controls and the two patients. In contrast, both patients and controls had comparable percentages of $CD4^+IFN\text{-}\gamma^+$ cells (Fig. 5).

Discussion

To our knowledge, this study shows for the first time that the de novo heterozygous mutation of c.1153C>T in exon 14 (p.T385M), affecting the DBD of STAT1, is the genetic cause of sporadic CMC in two unrelated Japanese patients. The underlying mechanisms involve gain of STAT1 function due to impaired STAT1 dephosphorylation, as observed in the CC domain mutations (4).

Recent extensive studies of the STAT1 molecule reveal the association between the mutations affecting DBD and gain of STAT1 function. Based on crystallographic analysis, Darnell's group (7, 8) proposed a model of reorientation of phosphorylated "parallel" STAT1 dimers to an "antiparallel" form after leaving the DNA, which allows for reciprocal association of the CC domain and a pocket residue of the DBD for dephosphorylation. They further demonstrated in direct mutagenesis experiments that mutations of the pocket residues of the DBD, Q340A or Q340W, G384A or G384W, and Q408A or Q408W, resulted in impaired dephosphorylation of STAT1 (8). The fact that T385, the amino acid altered in two of our patients, is evolutionarily conserved and is positioned next to the pocket residue G384 may indicate that it is also critical in the reciprocal association with the CC domain for stabilizing the antiparallel structure and for dephosphorylation. It is also possible that this mutation of the DBD leads to impaired dissociation from the DNA, which may also cause a resistance to dephosphorylation of the STAT1 molecule. Higher expression of total STAT1 in nuclear extracts from T385M/Wt and R274Q/Wt EBV-LCLs than from Wt EBV-LCLs may reflect impaired nuclear export due to a resistance to dephosphorylation of the mutant STAT1 molecule (18), although the precise mechanisms were not determined in this study.

There may be more patients with CMC who carry gain-of-function mutations affecting the DBD of STAT1, given that significant numbers of patients with *STAT1* mutations are reported from all over the world (4–6). Additionally, crystallographic analysis and mutagenesis studies showed that mutations in the N-terminal domain (aa 1–130) also resulted in persistent phosphorylation (7, 8). This suggests that mutations affecting the N-terminal domain may also be a genetic cause of CMC.

We demonstrated deficient Th17 cells (0.2% of $CD4^+$ cells) in Patient 1 with the heterozygous T385M mutation, which was similar to or more severe than the defect observed in Patient 3 with the heterozygous R274Q mutation (0.7% of $CD4^+$ cells). Deficient development of Th17 cells may explain the increased susceptibility to *Candida* infection. IFN-γ, IFN-α, and IL-27 are potent inhibitors of Th17 cell development via STAT1 in mice and/or humans (19–21). Therefore, gain of STAT1 function in response to IFN-γ, IFN-α, or IL-27, which was observed in our patients, could be associated with deficient Th17 cell development. However, it remains to be determined precisely how gain of STAT1 function leads to deficient Th17 cells.

It is unclear whether there are differences in the clinical spectrum or severity of the disease between patients with the DBD mutations and the CC domain mutations. It might be worth noting that the two patients with the DBD mutation of T385M developed bronchiectasis in their early childhood, and one of them eventually developed HLH; these have not been described in patients with CC domain mutations.

With regard to HLH, administration of an anti–IFN-γ Ab was recently shown to have a therapeutic effect in two murine models of human hereditary HLH: perforin-deficient and Rab27a-deficient mice (22). Careful evaluation of the results indicates that T385M could be associated with higher expression of STAT1p in response to various stimulations (Fig. 3). Therefore, CMC patients with the DBD mutation of T385M may be more susceptible to the conditions presumably associated with enhanced IFN-γ–STAT1 signals, such as HLH. Detailed investigations of the clinical spectrum of these two populations should be conducted.

Acknowledgments

We thank Dr. D.M. Stewart (Metabolism Branch, National Cancer Institute, National Institutes of Health, Bethesda, MD) for reviewing the manuscript, the patients and their families for participation in this study, and Dr. H. Kanegane (Department of Pediatrics, Graduate School of Medicine, University of Toyama, Toyama, Japan) for coordinating patient recruitment.

Disclosures

The authors have no financial conflicts of interest.

References

1. Kirkpatrick, C. H. 1994. Chronic mucocutaneous candidiasis. *J. Am. Acad. Dermatol.* 31: S14–S17.
2. Mathis, D., and C. Benoist. 2009. Aire. *Annu. Rev. Immunol.* 27: 287–312.
3. Coleman, R., and R. J. Hay. 1997. Chronic mucocutaneous candidosis associated with hypothyroidism: a distinct syndrome? *Br. J. Dermatol.* 136: 24–29.
4. Liu, L., S. Okada, X. F. Kong, A. Y. Kreins, S. Cypowyj, A. Abhyankar, J. Toubiana, Y. Itan, M. Audry, P. Nitschke, et al. 2011. Gain-of-function human STAT1 mutations impair IL-17 immunity and underlie chronic mucocutaneous candidiasis. *J. Exp. Med.* 208: 1635–1648.
5. van de Veerdonk, F. L., T. S. Plantinga, A. Hoischen, S. P. Smeekens, L. A. Joosten, C. Gilissen, P. Arts, D. C. Rosentul, A. J. Carmichael, C. A. Smits-van der Graaf, et al. 2011. STAT1 mutations in autosomal dominant chronic mucocutaneous candidiasis. *N. Engl. J. Med.* 365: 54–61.
6. Smeekens, S. P., T. S. Plantinga, F. L. van de Veerdonk, B. Heinhuis, A. Hoischen, L. A. Joosten, P. D. Arkwright, A. Gennery, B. J. Kullberg, J. A. Veltman, et al. 2011. STAT1 hyperphosphorylation and defective IL12R/IL23R signaling underlie defective immunity in autosomal dominant chronic mucocutaneous candidiasis. *PLoS ONE* 6: e29248.
7. Zhong, M., M. A. Henriksen, K. Takeuchi, O. Schaefer, B. Liu, J. ten Hoeve, Z. Ren, X. Mao, X. Chen, K. Shuai, and J. E. Darnell, Jr. 2005. Implications of an antiparallel dimeric structure of nonphosphorylated STAT1 for the activation-inactivation cycle. *Proc. Natl. Acad. Sci. USA* 102: 3966–3971.
8. Mertens, C., M. Zhong, R. Krishnaraj, W. Zou, X. Chen, and J. E. Darnell, Jr. 2006. Dephosphorylation of phosphotyrosine on STAT1 dimers requires extensive spatial reorientation of the monomers facilitated by the N-terminal domain. *Genes Dev.* 20: 3372–3381.
9. Nagashima, T., A. Miyanoshita, Y. Sakiyama, Y. Ozaki, A. C. Stan, and K. Nagashima. 2000. Cerebral vasculitis in chronic mucocutaneous candidiasis: autopsy case report. *Neuropathology* 20: 309–314.

10. Yamada, M., Y. Okura, Y. Suzuki, S. Fukumura, T. Miyazaki, H. Ikeda, S. I. Takezaki, N. Kawamura, I. Kobayashi, and T. Ariga. 2012. Somatic mosaicism in two unrelated patients with X-linked chronic granulomatous disease characterized by the presence of a small population of normal cells. *Gene* 497: 110–115.
11. Schreiber, E., P. Matthias, M. M. Müller, and W. Schaffner. 1989. Rapid detection of octamer binding proteins with 'mini-extracts', prepared from a small number of cells. *Nucleic Acids Res.* 17: 6419.
12. Nagamine, K., P. Peterson, H. S. Scott, J. Kudoh, S. Minoshima, M. Heino, K. J. Krohn, M. D. Lalioti, P. E. Mullis, S. E. Antonarakis, et al. 1997. Positional cloning of the APECED gene. *Nat. Genet.* 17: 393–398.
13. Finnish-German APECED Consortium. 1997. An autoimmune disease, APECED, caused by mutations in a novel gene featuring two PHD-type zinc-finger domains. *Nat. Genet.* 17: 399–403.
14. Ferwerda, B., G. Ferwerda, T. S. Plantinga, J. A. Willment, A. B. van Spriel, H. Venselaar, C. C. Elbers, M. D. Johnson, A. Cambi, C. Huysamen, et al. 2009. Human dectin-1 deficiency and mucocutaneous fungal infections. *N. Engl. J. Med.* 361: 1760–1767.
15. Glocker, E. O., A. Hennigs, M. Nabavi, A. A. Schäffer, C. Woellner, U. Salzer, D. Pfeifer, H. Veelken, K. Warnatz, F. Tahami, et al. 2009. A homozygous CARD9 mutation in a family with susceptibility to fungal infections. *N. Engl. J. Med.* 361: 1727–1735.
16. Puel, A., S. Cypowyj, J. Bustamante, J. F. Wright, L. Liu, H. K. Lim, M. Migaud, L. Israel, M. Chrabieh, M. Audry, et al. 2011. Chronic mucocutaneous candidiasis in humans with inborn errors of interleukin-17 immunity. *Science* 332: 65–68.
17. Sharfe, N., H. K. Dadi, M. Shahar, and C. M. Roifman. 1997. Human immune disorder arising from mutation of the alpha chain of the interleukin-2 receptor. *Proc. Natl. Acad. Sci. USA* 94: 3168–3171
18. McBride, K. M., C. McDonald, and N. C. Reich. 2000. Nuclear export signal located within theDNA-binding domain of the STAT1transcription factor. *EMBO J.* 19: 6196–6206.
19. Villarino, A. V., E. Gallo, and A. K. Abbas. 2010. STAT1-activating cytokines limit Th17 responses through both T-bet-dependent and -independent mechanisms. *J. Immunol.* 185: 6461–6471.
20. Ramgolam, V. S., Y. Sha, J. Jin, X. Zhang, and S. Markovic-Plese. 2009. IFN-beta inhibits human Th17 cell differentiation. *J. Immunol.* 183: 5418–5427.
21. Diveu, C., M. J. McGeachy, K. Boniface, J. S. Stumhofer, M. Sathe, B. Joyce-Shaikh, Y. Chen, C. M. Tato, T. K. McClanahan, R. de Waal Malefyt, et al. 2009. IL-27 blocks RORc expression to inhibit lineage commitment of Th17 cells. *J. Immunol.* 182: 5748–5756.
22. Pachlopnik Schmid, J., C. H. Ho, F. Chrétien, J. M. Lefebvre, G. Pivert, M. Kosco-Vilbois, W. Ferlin, F. Geissmann, A. Fischer, and G. de Saint Basile. 2009. Neutralization of IFNgamma defeats haemophagocytosis in LCMV-infected perforin- and Rab27a-deficient mice. *EMBO. Mol. Med.* 1: 112–124.

Molecular Genetics and Metabolism 107 (2012) 513–520

Contents lists available at SciVerse ScienceDirect

Molecular Genetics and Metabolism

journal homepage: www.elsevier.com/locate/ymgme

Long-term efficacy of hematopoietic stem cell transplantation on brain involvement in patients with mucopolysaccharidosis type II: A nationwide survey in Japan

Akemi Tanaka [a,*], Torayuki Okuyama [b], Yasuyuki Suzuki [c], Norio Sakai [d], Hiromitsu Takakura [e,f], Tomo Sawada [m], Toju Tanaka [b], Takanobu Otomo [d], Toya Ohashi [g], Mika Ishige-Wada [h], Hiromasa Yabe [e,f], Toshihiro Ohura [i], Nobuhiro Suzuki [j], Koji Kato [k], Souichi Adachi [l], Ryoji Kobayashi [m], Hideo Mugishima [h], Shunichi Kato [e,f]

[a] Department of Pediatrics, Osaka City University Graduate School of Medicine, Osaka, Japan
[b] Department of Clinical Laboratory Medicine, National Center for Child Health and Development, Tokyo, Japan
[c] Medical Education Department Center, Gifu University School of Medicine, Gifu, Japan
[d] Department of Pediatrics, Osaka University Graduate School of Medicine, Osaka, Japan
[e] Department of Cell Transplantation, Tokai University School of Medicine, Isehara, Japan
[f] Department of Pediatrics, Tokai University School of Medicine, Isehara, Japan
[g] Department of Gene Therapy, Institute of DNA Medicine, The Jikei University School of Medicine, Tokyo, Japan
[h] Department of Pediatrics and Child Health, Nihon University School of Medicine, Tokyo, Japan
[i] Department of Pediatrics, Sendai City Hospital, Sendai, Japan
[j] Department of Pediatrics, Sapporo Medical University Hospital, Sapporo, Japan
[k] Division of Hematology/Oncology, Children's Medical Center, Japanese Red Cross Nagoya Daiichi Hospital, Nagoya, Japan
[l] Department of Human Health Sciences, Kyoto University Graduate School of Medicine, Kyoto, Japan
[m] Department of Pediatrics, Sapporo Kitanire Hospital, Sapporo, Japan

ARTICLE INFO

Article history:
Received 1 September 2012
Accepted 1 September 2012
Available online 7 September 2012

Keywords:
Hematopoietic stem cell transplantation
Mucopolysaccharidosis type II
Brain efficacy
Survey

ABSTRACT

Hematopoietic stem cell transplantation (HSCT) has not been indicated for patients with mucopolysaccharidosis II (MPS II, Hunter syndrome), while it is indicated for mucopolysaccharidosis I (MPS I) patients <2 years of age and an intelligence quotient (IQ) of ≥70. Even after the approval of enzyme replacement therapy for both of MPS I and II, HSCT is still indicated for patients with MPS I severe form (Hurler syndrome). To evaluate the efficacy and benefit of HSCT in MPS II patients, we carried out a nationwide retrospective study in Japan. Activities of daily living (ADL), IQ, brain magnetic resonance image (MRI) lesions, cardiac valvular regurgitation, and urinary glycosaminoglycan (GAG) were analyzed at baseline and at the most recent visit. We also performed a questionnaire analysis about ADL for an HSCT-treated cohort and an untreated cohort (natural history). Records of 21 patients were collected from eight hospitals. The follow-up period in the retrospective study was 9.6 ± 3.5 years. ADL was maintained around baseline levels. Cribriform changes and ventricular dilatation on brain MRI were improved in 9/17 and 4/17 patients, respectively. Stabilization of brain atrophy was shown in 11/17 patients. Cardiac valvular regurgitation was diminished in 20/63 valves. Urinary GAG concentration was remarkably lower in HSCT-treated patients than age-matched untreated patients. In the questionnaire analysis, speech deterioration was observed in 12/19 patients in the untreated cohort and 1/7 patient in HSCT-treated cohort. HSCT showed effectiveness towards brain or heart involvement, when performed before signs of brain atrophy or valvular regurgitation appear. We consider HSCT is worthwhile in early stages of the disease for patients with MPS II.

1. Introduction

Hematopoietic stem cell transplantation (HSCT) is a standard therapy for young patients with mucopolysaccharidosis I (MPS I, Hurler syndrome, OMIM 607014) [1–4]. HSCT is indicated when MPS I patients are <2 years of age and show an intelligence quotient (IQ) of ≥70. However, HSCT has not been indicated for patients with mucopolysaccharidosis II (MPS II, Hunter syndrome, OMIM 309900) as no obvious efficacy has been shown on the brain involvement of MPS II patients [5–8].

Abbreviations: ADL, activities of daily living; DQ, development quotient; ERT, enzyme replacement therapy; FIM, functional independence measure; GAG, glycosaminoglycan; HSCT, hematopoietic stem cell transplantation; IQ, intelligence quotient; JSPH, Japanese Society for Pediatric Hematology; MPS, mucopolysaccharidosis; MRI, magnetic resonance imaging; SD, standard deviation.

* Corresponding author at: Department of Pediatrics, Osaka City University Graduate School of Medicine, 1-4-3 Asahi-machi, Abeno-ku, Osaka 545-8585, Japan. Fax: +81 6 6636 8737.
E-mail address: akemi-chan@med.osaka-cu.ac.jp (A. Tanaka).

1096-7192/$ – see front matter © 2012 Elsevier Inc. All rights reserved.
http://dx.doi.org/10.1016/j.ymgme.2012.09.004

Enzyme replacement therapy (ERT) for MPS II was approved in the USA and Europe in 2006, and in Japan in 2007. Its efficacy has been demonstrated for visceral organ and soft connective tissue involvement [9,10], but poor or no efficacy was observed for brain involvement [11,12] because of poor penetration across the blood–brain barrier. Poor efficacy has also been speculated towards hard connective tissues such as bone and heart valves because of poor vascularity. Moreover, weekly injection can prove inconvenient to patients and their families, and the high cost of treatment is another issue to be taken into consideration.

MPS II is the most frequent type of MPS in Asian patients, accounting for 60% of all MPS types in Japan. Before the approval of ERT, HSCT was indicated for MPS II as a standard therapy in Japan. The efficacy of HSCT on visceral organs was clear and similar to that of ERT [13]. However, efficacy on the brain or heart valves has not been clearly evaluated for either ERT or HSCT.

We present the results of a retrospective evaluation of the efficacy of HSCT on MPS II by collecting the clinical records of the patients with MPS II who received HSCT from 1990 to 2003. We also analyzed the answers to a questionnaire given to two cohorts: HSCT-treated and HSCT-untreated (natural history) MPS II patients.

2. Methods

2.1. MPS II classification

Disease severity was evaluated in all patients into four types (A–D) on the basis of chronological development, history of disease onset, initial symptoms, and clinical records before transplantation. Because of the wide spectrum of clinical phenotypes in MPS II, it is important to compare patients within the same type of disease for the evaluation of efficacy. Types A and B are attenuated forms with normal intelligence, while Types C and D are severe forms with mental impairment. MPS II was classified as follows:

- Type A is the most attenuated form. Onset is at school age with joint stiffness. Patients show normal intelligence, can go to and learn at a normal school, and work.
- Type B shows onset before school age with joint stiffness and/or abdominal distension. They show normal intelligence in primary school but hearing and physical impairments may impact development to a low degree in high school.
- Type C is a severe form. The abnormality is noted at ≥2 years of age. They start to speak words at 12–18 months of age and speak sentences at 2–3 years of age. Developmental delay and abnormal features become obvious after 3 years of age.
- Type D is a most severe form. The abnormality is noted at <2 years of age. Abnormal features are obvious around 1 year of age. Speech is definitely delayed. They start to speak words at ≥2 years of age (or may not speak), but sentences are never spoken.

2.2. Retrospective study from transplanted patients' records

This study was approved by the HSCT committee the Japanese Society of Pediatric Hematology (JSPH) and the ethics committees of the participating institutes.

A questionnaire was sent to 12 transplant centers in Japan to ask whether they had any type of MPS patients who had received HSCT and were surviving with donor cell engraftment and complete or incomplete chimera. We then mailed the physicians in charge of the patients with MPS II to obtain informed consent from the patients and/or their guardians so that data could be collected from their clinical records.

School status, movement and daily activities, conversation, and toileting were graded into Levels A (independent), B (assisted occasionally), C (assisted in every event), and D (bedridden, lack of communication, or wholly assisted) for each item from questionnaires and/or clinical records. Data on intelligence quotient (IQ) and development quotient (DQ) were also collected from clinical records. Functional independence measure (FIM) score was also analyzed and compared with the natural history of the disease as described in a previous report [14].

Brain magnetic resonance imaging (MRI) abnormalities were classified into four distinct types (Categories I–IV) and graded by scores according to a previous report [15]. The score was judged by two pediatricians and one radiologist. The categories were as follows:

- Category I. Cystic or cribriform lesions were graded from T1-weighted MRI as follows: 0 = none; 1 = mild (≤10 cystic lesions<3 mm); 2 = moderate (>10 small cystic lesions of<3 mm); and 3 = severe (many cystic lesions including those >3 mm).
- Category II. White matter signal changes observed on T2-weighted MRI were graded as follows: 0 = none; 1 = mild (a few limited to the periventricular area); and 2 = severe (in most parts of the periventricular area and other white matter areas).
- Category III. Ventricular enlargement was graded as follows: 0 = none; 1 = mild (<3 mm widening of the third ventricle without temporal horn dilatation); 2 = moderate, (>5–10 mm widening of the third ventricle); and 3 = severe (>10 mm dilatation of the third ventricle with bulbous configuration).
- Category IV. Brain atrophy was graded as follows: 0 = none, 1 = mild (mild widening of Sylvian and interhemispheric fissures by <3 mm, but not all of the sulci are involved); 2 = moderate (widening of all fissures and sulci by 3–5 mm); and 3 = severe (widening of all fissures and sulci by >5 mm with definite loss of cortex and white matter).

Cardiac valvular regurgitations were analyzed by color Doppler echocardiogram with each valve graded according to severity into four levels (I–IV) by the Sellers' classification [16].

Urinary glycosaminoglycan (GAG) was analyzed as the amount of uronic acid. These data were compared with the values in HSCT-untreated MPS II patients and also with those in ERT-treated MPS II patients.

2.3. Family questionnaire analysis

We sent a questionnaire to each of the 60 families with 66 MPS II patients registered with "the Japanese MPS Family Society". Information was collected about chronological development and course of deterioration for both HSCT-treated and HSCT-untreated (natural history) patients. Patients were first classified according to MPS II Types A–D on the basis of information on chronological development, before HSCT if performed, and at disease onset. Data were compared between HSCT-treated and HSCT-untreated patients for MPS II Type C or D patients.

3. Results

3.1. Retrospective study from transplanted patient records

Among transplanted patients with MPS, 63% (26/41) had MPS II. The 5-year survival rate after treatment of MPS II was 88.5% during the period from 1990 to 2003. Clinical records were collected for the 21 surviving patients (81%) from eight hospitals: Type A (n = 1), Type B (n = 6), Type C (n = 7), and Type D (n = 7) [Tables 1 and 2]. Donor state, transplantation protocol, and chimeric status are also summarized in Table 2. Two patients with Type B disease (patients 10-3 and 10-5) received total body irradiation (TBI) in the transplantation protocol. The donors for patients 10-7 and 7-6 were carrier siblings: patient 10-7 showed extremely low iduronate 2-sulfatase activity (25% of normal) even though complete chimera was obtained, while iduronate 2-sulfatase activity was normal in patient 7-6. Chimeric status was determined by short tandem repeats analysis in all patients except for four patients (patients 10-7, 7-8, 7-1, and 1-1) where sex chromosome was

Table 1
Patient numbers for each MPS II type and the results of HSCT effectiveness.

	No. of patients			
	Type A	Type B	Type C	Type D
Retrospective study from transplant patient records (n = 21)	1	6	7	7
ADL (see Table 2)				
Patients analyzed (n = 13)	1	3	5	4
Patients stabilized/improved from baseline	1	2	3	4
IQ/DQ (see Table 2)				
Patients analyzed (n = 11)	0	2	4	5
Patients stabilized/improved from baseline	0	2	1	0
FIM (see Table 2)				
Patients analyzed (n = 11)	1	1	6	3
Patients stabilized/improved from baseline	1	1	2	1
Brain MRI (see Tables 2 and 3)				
Patients analyzed (n = 17)	1	6	5	5
Patients stabilized/improved from baseline (see Tables 2 and 3)	0	5	4	2
Cardiac valvular regurgitation (see Tables 2 and 4)				
Patients analyzed (n = 21)	1	6	7	7
Patients stabilized/improved from baseline	1	4	5	6
Family questionnaire analysis (n = 60)	7	13	26 (see Table 5)	14
HSCT (+) (n = 17); [no. rejected]	3 [1]	3 [1]	7	4
HSCT (−) (n = 43)	4	10	19	10

Abbreviations: ADL, activities of daily living; DQ, development quotient; FIM, functional independence measure; IQ, intelligence quotient; MRI, magnetic resonance imaging.

analyzed. The activity of iduronate 2-sulfatase in patient 1-3 showed the lower limit of normal activity, probably because of incomplete chimera. All other patients showed activity within the mean ± 1 SD of normal. Age at transplantation was 64.2 ± 30.2 months. The mean follow-up period was 115.7 ± 41.4 months. Patient numbers for each MPS II type and a brief summary of results for HSCT effectiveness are shown in Table 1.

Clinical background and outcome among HSCT-treated MPS II patients are detailed in Table 2. Not every patient underwent all clinical examinations. Answers to the questionnaire were obtained for the analysis of ADL (school status, movement and daily activities, conversation, and toileting) from 13 patients: Type A (n = 1), Type B (n = 3), Type C (n = 5), and Type D (n = 4). Two patients with attenuated forms of the disease (patients 1-3 and 7-3) maintained a normal level of ADL (Level A) for each item throughout the observation period. None of the patients with severe forms of the disease except two Type C patients (patients 5-1 and 1-1) showed deterioration from baseline status.

IQ/DQ data were available for 11 patients: Type B (n = 2), Type C (n = 4), and Type D (n = 5). Two Type B patients (7-3 and 7-2) showed an IQ within the normal range both at baseline and at the most recent assessment. Deterioration was observed in two Type C patients (5-2 and 7-6) and two Type D patients (7-4 and 12-1). One Type C (patient 5-1) and one Type D (patient 8-2) showed such severe deterioration at baseline that evaluation of change was not possible. One Type C patient (7-1) and two Type D patients (7-5 and 9-1), whose IQ/DQ were > 70 at baseline, maintained their developmental status without deterioration, while DQ decreased with increasing age (Table 2).

FIM score was available in 11 patients: Type A (n = 1), Type B (n = 1), Type C (n = 6), and Type D (n = 3). Patients with Type A/B disease maintained scores in the normal range. Three Type C/D patients (7-8, 7-1, and 4-1) showed disease attenuation in FIM score when compared with the natural history described in a previous report [14]. One Type C (patient 7-8) and one Type D (patient 4-1) showed disease attenuation in FIM score for motor function, while the score for cognition did not differ from untreated patients. One Type C (patient 7-1) showed disease attenuation in FIM scores for both motor function and cognition. Other patients with severe forms of the disease (4 Type C and 2 Type D) showed no difference as compared to the previously reported untreated patients [14]. The results are summarized in Table 2.

IQ/DQ and FIM scores were both obtained in seven patients: one Type B (patient 7-2), four Type C (patients 5-2, 7-6, 7-1, and 5-1), and two Type D (9-1 and 12-1). Among these patients with Type C/D disease and brain involvement, only one patient (7-1) showed disease attenuation in both FIM score and developmental status. The remaining three Type C patients showed no difference in FIM score as compared to natural history. While developmental status and ADL improved in patient 9-1, no efficacy in FIM score was shown as compared to natural history.

Brain MRI data were analyzed in 17 patients: Type A (n = 1), Type B (n = 6), Type C (n = 5), and Type D (n = 5) [Table 2]. Improvements in Categories I and III lesions were shown in nine (4 Type B, 2 Type C, and 3 Type D) and four patients (2 Type C and 2 Type D), respectively. Eight out of 17 patients (59%) had an improvement in total score. All of the six patients who showed an increase in total score had deterioration in Category IV lesions (brain atrophy). Three of these six patients had Type D disease (patients 7-4, 8-2, and 10-1). Two patients (7-1 and 4-1) who showed disease attenuation in FIM score also showed improvement in brain MRI abnormality scores. There was no difference in the effectiveness between the attenuated forms (Type A/B) and severe forms (Type C/D) of the disease or any correlation between the effectiveness of HSCT and age at HSCT, as summarized in Table 3.

Valvular regurgitation was analyzed for mitral, aortic, and tricuspid valves. Pulmonary valves showed insufficient lesions to warrant analysis. Twenty-one patients were analyzed: Type A (n = 1), Type B (n = 6), Type C (n = 7), and Type D (n = 7), i.e. a total of 63 valves. Results are summarized in Tables 2 and 4. Valvular regurgitation improved in 32% and stabilized in 56% of valves. There was no difference in efficacy between patients with the attenuated (Type A/B) and severe forms (Type C/D) of MPS II (data not shown). However, valvular regurgitation deteriorated more frequently in the patients transplanted at ≥6 years of age (5 valves out of 8 patients), as shown in Table 4.

The amount of urinary GAG was analyzed from urinary uronic acid concentrations. Mean urinary uronic acid concentrations in children ages 7–16 years were 18.0 ± 5.5 (n = 24) and 165.5 ± 77.9 (n = 9) mg/g creatinine for normal children and among untreated Types A–D MPS II patients, respectively. Urinary GAG in HSCT-treated MPS II patients was 24.8 ± 9.8 mg/g creatinine (n = 7, ages 9–17 years). Urinary GAG in ERT-treated patients with MPS II at Osaka City University Hospital was 37.6 ± 14.3 mg/g creatinine (n = 6, age 7–16 years).

3.2. Family questionnaire analysis

Answers to the questionnaire were collected for 60 patients with MPS II from 55 families. The numbers of HSCT-treated and HSCT-untreated patients were 17 and 43, respectively. As the questionnaire sheet was anonymous, we could not identify the patients analyzed in the clinical study described above. The patients were divided into Types A–D clinical forms (Table 1), as previously described. Six out of 20 Type A/B patients were treated by HSCT and two of them (one each with Types A and B) underwent rejection. Four of 14 Type D patients received HSCT. However, they showed deterioration before transplantation. We analyzed the efficacy of HSCT in 26 Type C patents with respect to disease progression by age at onset of speech deterioration, walking disability, and convulsion (Table 5). The numbers of patients in the HSCT-treated and HSCT-untreated cohorts were 7 and 19, respectively. Mean ages of these cohorts were 145.7 ± 67.8 and 142.7 ± 88.6 months, respectively.

Seven Type C patients underwent HSCT at a mean age of 65.9 ± 22.1 months (range, 44–111 months). Before HSCT treatment, the seven patients showed no difference in developmental milestones as compared to the 19 HSCT-untreated patients. At the time of survey, 12 out of 19 (63%) HSCT-untreated patients showed deterioration of

Table 2
Clinical background and outcome among HSCT-treated MPS II patients (n = 21).

Patient no.	Disease type	Age at HSCT	Donor	Protocol	Chimeric status	GVHD	Follow-up	ADL (pre/post), [n = 13]				IQ/DQ (developmental age)	
								School status	Movement and daily activities	Conversation	Toileting	Pre	Post
1-3	A	19 y 8 m	Unrelated BM	CY + BU + ATG	50	No	6 y 7 m	(A/A)	(A/A)	(A/A)	(A/A)	NA	
10-3	B	4 y 11 m	Unrelated CB	CY + TBI	100	No	7 y 1 m	NA	NA	NA	NA	NA	
7-3	B	5 y 5 m	Normal sibling	CY + BU + ATG	100	No	8 y 7 m	(A/A)	(B/A)	(A/A)	(A/A)	114 (normal)	102 (normal)
7-2	B	6 y 0 m	Normal sibling	BU + ATG	Mixed	No	10 y 11 m	NA	NA	NA	NA	99 (normal)	91 (normal)
8-1	B	9 y 5 m	Normal sibling	CY + BU	100	No	12 y 7 m	(E/E)	(E/E)	(B/B)	(E/E)	NA	
10-7	B	7 y 9 m	Carrier sibling	CY + BU + ATG	100	No	11 y 3 m	(A/A)	(A/A)	(A/A)	(A/A)	NA	
10-5	B	11 y 6 m	Unrelated BM	CY + TBI	90	Yes	6 y 6 m	(A/D)*	(B/B)	(A/A)	(A/A)	NA	
5-2	C	3 y 4 m	Normal sibling	CY + BU	100	No	7 y 4 m	(B/B)	(C/B)	(B/B)	(D/B)	53 (3 y 11 m)	NA
7-8	C	4 y 3 m	Unrelated BM	CY + BU + ATG	100	No	7 y 4 m	NA	NA	NA	NA	NA	
7-7	C	5 y 5 m	Unrelated CB	CY + BU + ATG	100	No	7 y 7 m	NA	NA	NA	NA	NA	
7-6	C	5 y 9 m	Carrier sibling	CY + BU + ATG	100	No	6 y 11 m	(B/B)	(C/C)	(D/C)	(D/B)	25 (1 y 8 m)	NA
7-1	C	7 y 0 m	Normal sibling	CY + BU	100	Yes	16 y 3 m	(B/B)	(B/A)	(B/A)	(E/E)	78 (5 y 6 m)	65 (9 y 6 m)
5-1	C	7 y 3 m	Normal sibling	CY + BU	100	No	10 y 5 m	(B/B)	(C/D)*	(C/C)	(B/C)*	NA	NA
1-1	C	9 y 4 m	Normal sibling	CY + BU	100	No	16 y	(C/D)*	(C/D)*	(C/D)*	(C/D)*	NA	
7-4	D	2 y 0 m	Unrelated BM	CY + BU + ATG	100	Yes	9 y 11 m	NA	NA	NA	NA	50 (1 y 0 m)	NA
7-5	D	2 y 2 m	Normal sibling	CY + BU + ATG	96	No	8 y 8 m	NA	NA	NA	NA	70 (1 y 6 m)	29 (2 y 2 m)
9-1	D	2 y 2 m	Unrelated BM	CY + BU + ATG	100	No	12 y	(E/B)	(C/A)	(B/A)	(C/A)	100 (2 y 2 m)	40 (5 y 6 m)
12-1	D	2 y 6 m	Normal sibling	CY + BU	100	No	8 y 3 m	(E/B)	(C/C)	(C/C)	(D/D)	66 (5 y 6 m)	30 (1 y 10 m)
8-2	D	2 y 9 m	Normal sibling	CY + BU	100	No	12 y 3 m	(D/B)	(D/D)	(D/D)	(D/D)	NA	NA
4-1	D	4 y 2 m	Unrelated BM	CY + BU + ATG	100	No	5 y 5 m	(B/B)	(A/A)	(C/B)	(D/B)	NA	
10-1	D	5 y 4 m	Normal sibling	CY + BU + ATG	100	No	7 y 8 m	NA	NA	NA	NA	NA	

Abbreviations: ADL, activities of daily living; ATG, antithymocyte globulin; BM, bone marrow; BU, busulfan; CB, cord blood; CY, cyclophosphamide; DQ, development quotient; FIM, functional independence measure; HSCT, hematopoietic stem cell transplantation; IQ, intelligence quotient; m, month; MPS, mucopolysaccharidosis; MRI, magnetic resonance imaging; NA, not available (not found, not examined, and/or not measurable); TBI, total body irradiation; y, year.

[a] Regression of level or score.

Table 2 (*continued*)

Patient no.	FIM	Brain MRI abnormality (pre/post) [n = 17]				Valvular regurgitation (pre/post) [n = 21]		
	Difference from natural history	Category I (cribriform change)	Category II (white matter signal change)	Category III (ventricular enlargement)	Category IV (brain atrophy)	Mitral	Aortic	Tricuspid
1-3	Normal range	(2/2)	(1/2)[a]	(2/2)	(1/2)[a]	II–III/IV	II/I	II–III/IV
10-3	Normal range	(1.5/0.5)	(0/0)	(1/1)	(0/0)	III/(−)	(−)/(−)	(−)/(−)
7-3	NA	(1/0.5)	(0/0)	(0/0)	(0/0)	I–II/(−)	II/(−)	(−)/(−)
7-2	Normal range	(1/0)	(0/0)	(0/0)	(0/0)	I–II/I–II	(−)/II[a]	I/(−)
8-1	NA	(1/1)	(2/2)	(1/1)	(0/0)	I/I	(−)/II[a]	I/I
10-7	NA	(3/2)	(0/0)	(0/0)	(0/0)	II/I	(−)/(−)	(−)/(−)
10-5	NA	(1/2)[a]	(0/0)	(0/1)	(0.5/1.5)[a]	I/I	II/II	(−)/(−)
5-2	No difference	NA	NA	NA	NA	(−)/(−)	(−)/(−)	(−)/(−)
7-8	Attenuation	(1/1)	(0/0)	(0/0)	(0/0)	I/I	(−)/(−)	I/I
7-7	NA	(1/0)	(1/0)	(1/0)	(0/0)	III/II–III	(−)/II[a]	I/(−)
7-6	No difference	(1/1)	(0/0)	(2/2)	(1/1.5)[a]	(−)/(−)	II/(−)	II/(−)
7-1	Attenuation	(1/0)	(0/0)	(2/1.5)	(1/1)	I/I	I/(−)	(−)/(−)
5-1	No difference	NA	NA	NA	NA	(−)/I[a]	II/I	(−)/(−)
1-1	No difference	(2/2)	(2/2)	(2/2)	(3/3)	I/II[a]	II/I	(−)/(−)
7-4	NA	(0.5/0)	(0/0)	(0/1)[a]	(0/1)[a]	II/I	II/I	I/(−)
7-5	NA	(1/0)	(0/0)	(0.5/0)	(0/0)	II/II	(−)/(−)	(−)/(−)
9-1	No difference	NA	NA	NA	NA	(−)/II[a]	I/I	(−)/(−)
12-1	No difference	NA	NA	NA	NA	(−)/(−)	(−)/(−)	(−)/(−)
8-2	NA	(2/2)	(1/1)	(1/2)[a]	(2/3)[a]	(−)/(−)	(−)/III[a]	I/(−)
4-1	Attenuation	(1/0.5)	(0/0)	(1/0.5)	(0/0)	(−)/(−)	I/I	(−)/(−)
10-1	NA	(0.5/0.5)	(0/0)	(3/3)	(2/3)[a]	(−)/(−)	(−)/(−)	(−)/(−)

Table 3
Effectiveness of HSCT on brain MRI lesions among MPS II patients according to age at transplantation or MPS II clinical classification.

	No. of patients					
	Age at HSCT				MPS II classification	
	<4 y (n=3)	4–5 y (n=3)	5–6 y (n=5)	>6 y (n=6)	Type A/B (n=7)	Type C/D (n=10)
Improved (n=8)	1	2	3	2	4	4
Stable (n=3)	0	1	1	2	1	2
Deteriorated (n=6)	2	0	2	2	2	4

Abbreviations: HSCT, hematopoietic stem cell transplantation; MPS, mucopolysaccharidosis, y, year.

speech, nine (47%) spoke no words, six (32%) had convulsions, and six (32%) did not walk. All but one of the HSCT-treated Type C patients showed no speech deterioration, loss of speech, or convulsions.

4. Discussion

We performed a retrospective study on the long-term efficacy of HSCT in MPS II patients. Efficacy was noted, to some extent, even with respect to brain involvement as long as HSCT was carried out before developmental delay became clinically manifest, without brain atrophy on MRI. The study of ADL from transplanted patient records showed that HSCT-treated patients maintained almost the same levels of speech ability and gait as at baseline or an improvement in most patients (Table 2). The questionnaire study among Type C patients of HSCT-treated and HSCT-untreated cohorts showed no deterioration in all except one Type C patient in the HSCT-treated cohort, which is different from the natural history of the disease (HSCT-untreated cohort) [Table 5]. However, no difference was shown in FIM score when compared to the natural history of the disease except for three patients (7-8, 7-1, and 4-1). Moreover, two patients with Type D disease (patients 7-5 and 9-1) with baseline DQ of 70 and 100, respectively, showed severe deterioration and no difference was shown with respect to the natural history of the disease for patient 9-1 with respect to FIM score. Thus, HSCT may not be effective with respect to brain involvement for Type D MPS II patients.

The effectiveness of HSCT on brain MRI was distinctive. Improvement in Categories I and III lesions was clearly shown. Category I lesions involve enlargement of perivascular spaces where GAG-loaded cells are accumulated and Category III lesions occur from insufficient cerebrospinal fluid absorption or secondarily from brain atrophy. It is speculated that engrafted cells migrate into perivascular and subarachnoid spaces and secrete the deficient enzyme responsible for diminishing GAG storage, thereby improving lesions. On the other hand, for Category IV lesions, which results from neuronal cell loss, deterioration was observed in six patients and none improved. It may be that engrafted cells are not located to deep brain tissue. Of these six patients, three were Type D patients and two of them showed a worsening of Category III lesions, which probably resulted from the progression of Category IV lesions (brain atrophy). Thus, the efficacy of HSCT is not shown in Type D patients from the brain MRI study.

Two patients with Type C/D disease (patients 7-1 and 4-1) showed effectiveness in both intellectual (ADL, IQ/DQ, and FIM) and imaging analysis (brain MRI), while three patients (patients 7-6, 7-4, and 8-2) showed deterioration in both. These three patients already had severe intellectual deterioration at baseline with low IQ/DQ. However, no clear correlation between the effectiveness on brain MRI lesions and on intellectual scores was shown in other Type C/D patients because of insufficient data.

The most serious cardiac consequence in MPS II is valvular insufficiency. Thickening of heart valves by GAG accumulation and fibrosis results in valvular stenosis and regurgitation, culminating in heart failure, which is one of the most frequent causes of death in MPS II patients in our experience. Mitral valves and aortic valves were those primarily affected in our patients. In particular, the aortic perivalvular area was enlarged in older patients and caused regurgitation. Eighty-eight percent of valves showed improvement (32%) or stabilization (56%) with respect to regurgitation. A deterioration of valvular regurgitation was frequently observed in older patients who received HSCT, who already had regurgitation on baseline examination prior to engraftment. We have experience with different patients in a family with Type B MPS II who received and did not receive HSCT in this study. An uncle did not receive any therapy, could not walk at 17 years, and died at 20 years from heart failure. His nephew was 18 years at survey (patient 10-7) and underwent HSCT at 7 years and 9 months old. Although he had mitral valve regurgitation, he remained relatively well and was practicing kendo in high school. The efficacy of HSCT on the respiratory system probably reduced his cardiac stress.

Table 4
Changes in cardiac valve involvement according to age at HSCT among MPS II patients.

	No. of patients with cardiac valvular regurgitation (n=21)				
	Age at HSCT				
	<4 y (n=6)	4–5 y (n=3)	5–6 y (n=4)	≥6 y (n=8)	Total (n=21)
Mitral valve (n=21)					
Diminished	1	1	2	3	7 (33%)
Stable	4 [3[a]]	2 [1[a]]	2 [2[a]]	3 [0[a]]	11 [6[a]] (52%)
Increased	1	0	0	2	3 (14%)
Aortic valve (n=21)					
Diminished	1	0	2	4	7 (33%)
Stable	4 [3[a]]	3 [2[a]]	1 [1[a]]	1 [0[a]]	9 [6[a]] (43%)
Increased	1	0	1	3	5 (24%)
Tricspid valve (n=21)					
Diminished	2	0	2	2	6 (29%)
Stable	4 [4[a]]	3 [2[a]]	2 [2[a]]	6 [5[a]]	15 [13[a]] (71%)
Increased	0	0	0	0	0 (0%)
Total (n=63)					
Diminished	4	1	6	9	20 (32%)
Stable	12 [10[a]]	8 [5[a]]	5 [5[a]]	12 [6[a]]	35 [25[a]] (56%)
Increased	2	0	1	5	8 (13%)

Abbreviations: HSCT, hematopoietic stem cell transplantation; MPS, mucopolysaccharidosis; y, year.
[a] Number with absence of regurgitation at HSCT (baseline).

Table 5
Clinical course of HSCT-untreated and HSCT-treated Type C MPS II patients in questionnaire analysis.

	Pre-treatment in HSCT-treated cohort (n=7)	HSCT-untreated cohort (n=19)
Mean ± SD age at developmental milestones (m)		
Speak words	17.1 ± 4.1	18.0 ± 6.3
Speak sentences	32.0 ± 9.2	40.1 ± 14.2
Age when noticed developmental delay (m)	26.4 ± 16.6	34.2 ± 12.5
Mean ± SD age at HSCT (m)	65.9 ± 22.1	–
Mean ± SD age at survey (m)	145.7 ± 67.8	142.7 ± 88.6

Disease progression	Post-treatment in HSCT-treated cohort		HSCT-untreated cohort	
	No. of affected (%)	Age when noticed (m)	No. of affected (%)	Mean ± SD age when noticed (m)
Speech deterioration	1*/7 (14%)	42	12/19 (63%)	113.5 ± 40.4
Loss of speech	1*/7 (14%)	72	9/19 (47%)	150.4 ± 55.1
Convulsions	1*/7 (14%)	125	6/19 (32%)	186.0 ± 71.2
Unable to walk	0/7 (0%)	–	6/19 (32%)	186.5 ± 52.9

1*. The same patient.
Abbreviations: HSCT, hematopoietic stem cell transplantation; m, month; MPS, mucopolysaccharidosis; NA, not applicable; SD, standard deviation.

It is known that the efficacy of HSCT is affected by the transplantation condition. TBI can sometimes result in brain atrophy or dementia after many years delay. Since none of the Type C/D patients received TBI as part of their transplantation protocol, their deterioration must have resulted from the disease itself and not a consequence of TBI. It has been recently reported that lower enzyme activity after HSCT results in lower efficacy in the patients with MPS I severe form (Hurler syndrome) in a multicenter survey study of 197 patients [17]. In our study, two patients showed extremely low enzyme activity after HSCT. However, it is unclear whether they had poor efficacy from HSCT.

ERT has recently become available in Japan. It has demonstrated clear efficacy with respect to visceral organ involvement and urinary GAG secretion [9,10]. ERT is superior to HSCT in terms of safety and availability. However, ERT requires weekly injection, its cost is high, and antibody development is another problem. Moreover, the efficacy of ERT has not been clearly demonstrated with respect to brain [11,12] or heart valve involvement.

In patients who received HSCT, urinary GAG concentration was definitely decreased after engraftment. Values became almost the same as those of normal children. In ERT-treated MPS II patients, however, urinary GAG concentration was slightly higher than that in HSCT-treated patients. Similar results have been previously reported in patients with MPS I [4]. It is possible that engrafted cells provide the deficient enzyme more efficiently to the affected cells and organs than by systemic ERT administration.

In contrast to the efficacy of HSCT with respect to MRI findings, our personal experience with ERT of six patients aged 1–12 years with severe MPS II showed a 4%–12% brain volume reduction following 2 years' treatment (data not shown). Moreover, none of them showed any improvement in any MRI lesion category. However, Wang et al. [18] reported that ERT reduced or stabilized brain MRI abnormalities. Longer observation periods are necessary to evaluate the efficacy of ERT on ADL, and heart and brain involvement.

Our study showed an improvement of brain MRI findings in HSCT-treated patients. We speculate that the efficacy is due to migrated microglial cells derived from donor cells. In 2009, Araya et al. [19] reported the localization of donor cells in the brain of a patient with MPS II after cord blood cell transplantation. Several studies have shown the migration of transplanted bone marrow cells into brain tissue [20,21]. In a recent report, autologous cord blood infusion showed some efficacy in children with acquired neurologic disorders [22]. It is known that HSCT shows efficacy on brain involvement in patients with genetic leukodystrophies including adrenoleukodystrophy, metachromatic leukodystrophy, and globoid cell leukodystrophy [23], and HSCT is a standard therapy for these patients in early stages of the disease. HSCT combined with gene therapy (ex vivo gene therapy) using a lentiviral vector has recently been shown to be successful in two patients with adrenoleukodystrophy [24]. It is speculated that stem cells can migrate across the blood–brain barrier in some situations such as the environment induced by disease.

On the other hand, the efficacy of HSCT on IQ/DQ was unclear in patients with MPS II. However, it can be concluded that the disease of lesser severity and an earlier time of transplantation will lead to better efficacy on IQ/DQ.

The disadvantages of HSCT are the mortality (11.5% in 1990–2003) and morbidity associated with the transplantation procedure [25]. Suitable donors may not be found easily and quickly. However, once engraftment has been established, the quality of life of patients will be better than in patients receiving weekly ERT treatment. Moreover, the expense of HSCT is less than that for ERT. HSCT also improves morbidity in patients with MPS II, particularly when performed early in the course of the disease. Exogenous ERT is unable to correct cognitive and CNS disease because of its inability to cross the blood–brain barrier. In contrast, HSCT allows donor-derived, enzyme-producing cells to migrate into the brain and other organs, thereby providing a permanent form of enzyme replacement [26,27]. The utility of HSCT should therefore be re-evaluated in the treatment for MPS II. HSCT is a worthwhile treatment for MPS II when it is performed before signs of brain atrophy appear on MRI and before heart valvular regurgitation appear. Therefore, neonatal screening for MPS II may result in improving of the prognosis. In the future, genetically engineered bone marrow cells, autologous cord blood cells, or other cells may become good sources for cell transplantation, or other novel intervention for genetic diseases may be developed.

Conflict of interest

Each author declares no potential conflict of interest, real or perceived.

Acknowledgments

We indebted to the patients and families of the members in The Japanese MPS Family Society for providing answers to the questionnaire. We thank Ms. Miho Tabe in SRL Clinical Laboratory Inc. for providing the data on uronic acid concentrations in HSCT-treated patients. We also thank Drs. Toru Yorifuji, Hiraku Doi, and Takeo Kato, Department of Pediatrics, Kyoto University Graduate School of Medicine, for collecting data from historic clinical records and Dr. Yukio Miki, Department of Radiology, Osaka City University Graduate School of Medicine, for expert advice on evaluating MRI lesions.

This study was supported by grant H20-Clinical Study General-011, and the matching fund subsidy of "Research on Measures for Intractable Diseases" project from the Ministry, of Health, Labour and Welfare, Japan.

References

[1] J.R. Hobbs, K. Hugh-Jones, A.J. Barrett, N. Byrom, D. Chambers, K. Henry, D.C. James, C.F. Lucas, T.R. Rogers, P.F. Benson, L.R. Tansley, A.D. Patrick, J. Mossman, E.P. Young, Reversal of clinical features of Hurler's disease and biochemical improvement after treatment by bone-marrow transplantation, Lancet 2 (1981) 709–712.

[2] S.L. Staba, M.L. Escolar, M. Poe, Y. Kim, P.L. Martin, P. Szabolcs, J. Allison-Thacker, S. Wood, D.A. Wenger, P. Rubinstein, J.J. Hopwood, W. Krivit, J. Kurtzberg, Cord-blood transplants from unrelated donors in patients with Hurler's syndrome, N. Engl. J. Med. 350 (2004) 1960–1969.

[3] J.J. Boelens, R.F. Wynn, A. O'Maera, P. Veys, Y. Bertrand, G. Souillet, J.E. Wraith, A. Fischer, M. Cavazzana-Calvo, K.W. Sykora, P. Sedlacek, A. Rovelli, C.S. Uiterwaal, N. Wulffraat, Outcomes of hematopoietic stem cell transplantation for Hurler's syndrome in Europe: a risk factor analysis for graft failure, Bone Marrow Transplant. 40 (2007) 225–233.

[4] J. Muenzer, J.E. Wraith, L.A. Clarke, Mucopolysaccharidosis I: management and treatment guidelines, Pediatrics 123 (2009) 19–29.

[5] N. Guffon, Y. Bertrand, I. Forest, A. Fouilhoux, R. Froissart, Bone marrow transplantation in children with Hunter Syndrome: outcome after 7 to 17 years, J. Pediatr. 154 (2009) 733–737.

[6] E.J. McKinnis, S. Sulzbacher, J.C. Rutledge, J. Sanders, C.R. Scott, Bone marrow transplantation in Hunter syndrome, J. Pediatr. 129 (1996) 145–148.

[7] A. Vellodi, E. Young, A. Cooper, V. Lidchi, B. Winchester, J.E. Wraith, Long-term follow-up following marrow transplantation for Hunter disease, J. Inherit. Metab. Dis. 22 (1999) 638–648.

[8] C. Peters, W. Krivit, Hematopoietic cell transplantation for mucopolysaccharidosis IIB (Hunter syndrome), Bone Marrow Transplant. 25 (2000) 1097–1099.

[9] J.E. Wraith, M. Scarpa, M. Beck, O.A. Bodamer, L. De Meirleir, N. Guffon, A. Meldgaard Lund, G. Malm, A.T. Van der Ploeg, J. Zeman, Mucopolysaccharidosis type II (Hunter syndrome): a clinical review and recommendations for treatment in the era of enzyme replacement therapy, Eur. J. Pediatr. 167 (2008) 267–277.

[10] T. Okuyama, A. Tanaka, Y. Suzuki, H. Ida, T. Tanaka, G.F. Cox, Y. Eto, T. Orii, Japan Elaprase Treatment (JET) study: idursulfase enzyme replacement therapy in adult patients with attenuated Hunter syndrome (mucopolysaccharidosis II, MPS II), Mol. Genet. Metab. 99 (2010) 18–25.

[11] F. Papadia, M.S. Lozupone, A. Gaeta, D. Capodiferro, G. Lacalendola, Long-term enzyme replacement therapy in a severe case of mucopolysaccharidosis type II (Hunter syndrome), Eur. Rev. Med. Pharmacol. Sci. 15 (2011) 253–258.

[12] R. Manara, E. Priante, M. Grimaldi, L. Santoro, L. Astarita, R. Barone, D. Concolino, M. Di Rocco, M.A. Donati, S. Fecarotta, A. Ficcadenti, A. Fiumara, F. Furlan, I. Giovannini, F. Lilliu, R. Mardari, G. Polonara, E. Procopio, A. Rampazzo, A. Rossi, G. Sanna, R. Parini, M. Scarpa, Brain and spine MRI features of Hunter disease: frequency, natural evolution and response to therapy, J. Inherit. Metab. Dis. 34 (2011) 763–780.

[13] M. Imaizumi, K. Gushi, I. Kurobane, S. Inoue, J. Suzuki, Y. Koizumi, H. Suzuki, A. Sato, Y. Gotoh, K. Haginoya, M. Kikuchi, J. Aikawa, K. Narisawa, A. Ohunuma, K. Ohmura, H. Shintaku, A. Tanaka, K. Tada, Long-term effects of bone marrow transplantation for inborn errors of metabolism: a study of four patients with lysosomal storage disease, Acta Pediatr. Jpn. 36 (1994) 30–36.
[14] T. Kato, Z. Kato, I. Kuratsubo, T. Ota, T. Orii, N. Kondo, Y. Suzuki, Evaluation of ADL in patients with Hunter disease using FIM score, Brain Dev. 29 (2007) 298–305.
[15] T. Seto, K. Kono, K. Morimoto, Y. Inoue, H. Shintaku, H. Hattori, O. Matsuoka, T. Yamano, A. Tanaka, Brain magnetic resonance imaging in 23 patients with mucopolysaccharidosis and the effect of bone marrow transplantation, Ann. Neurol. 50 (2001) 79–92.
[16] R.D. Sellers, M.J. Levy, K. Amplatz, C.W. Lillehei, Left retrograde cardioangiography in acquired cardiac disease: technique, indication and interpretations in 700 cases, Am. J. Cardiol. 14 (1964) 437–447.
[17] J. Boelens, M. Aldenhoven, M.L. Escolar, M.D. Poe, R.F. Wynn, A.O. Maera, A. Rovel, P. Veys, P. Orchard, J. Kurtzberg, J. Boelens, International multicenter study to identify predictors of long term outcome of Hurler syndrome patients after successful hematopoietic stem cell transplantation, in: Abstract S08.7 presented at the 12th International Symposium on MPS and Related Diseases, Noodwijkerhout, The Netherlands, Jun 28– Jul 1 2012.
[18] R.Y. Wang, E.J. Cambray-Forker, K. Ohanian, D.S. Karlin, K.K. Covault, P.H. Schwartz, J.E. Abdenur, Treatment reduces or stabilizes brain imaging abnormalities in patients with MPS I and II, Mol. Genet. Metab. 98 (2009) 406–411.
[19] K. Araya, N. Sakai, I. Mohri, K. Kagitani-Shimono, T. Okinaga, Y. Hashii, H. Ohta, I. Nakamichi, K. Aozasa, M. Taniike, K. Ozono, Localized donor cells in brain of a Hunter disease patient after cord blood stem cell transplantation, Mol. Genet. Metab. 98 (2009) 255–263.
[20] D.W. Kennedy, J.L. Abkowitz, Kinetics of central nervous system microglia and macrophage engraftment: analysis using a transgenic bone marrow transplantation model, Blood 90 (1997) 986–993.
[21] P. Sano, A. Tessitore, A. Ingrassia, A. d'Azzo, Chemokine-induced recruitment of genetically modified bone marrow cells into the CNS of GM1-gangliosidosis mice corrects neuronal pathology, Blood 106 (2005) 2259–2268.
[22] J. Sun, J. Allison, C. McLaughlin, L. Sledge, B. Waters-Pick, S. Wease, J. Kurtzberg, Differences in quality between privately and publicly banked umbilical cord blood units: a pilot study of autologous cord blood infusion in children with acquired neurologic disorders, Transfusion 50 (2010) 1980–1987.
[23] A. Gassas, J. Raiman, L. White, T. Schechter, J. Clarke, J. Doyle, Long-term adaptive functioning outcomes of children with inherited metabolic and genetic diseases treated with hematopoietic stem cell transplantation in a single large pediatric center: parents' perspective, J. Pediatr. Hematol. Oncol. 33 (2011) 216–220.
[24] N. Cartier, S. Hacein-Bey-Abina, C.C. Bartholomae, P. Bougnères, M. Schmidt, C.V. Kalle, A. Fischer, M. Cavazzana-Calvo, P. Aubourg, Hematopoietic stem cell gene therapy with a lentiviral vector in X-linked adrenoleukodystrophy, Science 326 (2009) 818–823.
[25] V.K. Prasad, A. Mendizabal, S.H. Parikh, P. Szabolcs, T.A. Driscoll, K. Page, S. Lakshminarayanan, J. Allison, S. Wood, D. Semmel, M.L. Escolar, P.L. Martin, S. Carter, J. Kurtzberg, Unrelated donor umbilical cord blood for inherited metabolic disorders in 159 pediatric patients from a single center: influence of cellular composition of the graft on transplantation outcomes, Blood 112 (2008) 2979–2989.
[26] V.K. Prasad, J. Kurtzberg, Emerging trends in transplantation of inherited metabolic diseases, Bone Marrow Transplant. 4 (2008) 99–108.
[27] V.K. Prasad, J. Kurtzberg, Cord blood and bone marrow transplantation in inherited metabolic diseases: scientific basis, current status and future directions, Br. J. Haematol. 148 (2010) 356–372.

Frequent somatic mosaicism of *NEMO* in T cells of patients with X-linked anhidrotic ectodermal dysplasia with immunodeficiency

Tomoki Kawai,[1] Ryuta Nishikomori,[1] Kazushi Izawa,[1] Yuuki Murata,[1] Naoko Tanaka,[1] Hidemasa Sakai,[1] Megumu Saito,[2] Takahiro Yasumi,[1] Yuki Takaoka,[1] Tatsutoshi Nakahata,[2] Tomoyuki Mizukami,[3] Hiroyuki Nunoi,[3] Yuki Kiyohara,[4] Atsushi Yoden,[5] Takuji Murata,[5] Shinya Sasaki,[6] Etsuro Ito,[6] Hiroshi Akutagawa,[7] Toshinao Kawai,[8] Chihaya Imai,[9] Satoshi Okada,[10] Masao Kobayashi,[10] and Toshio Heike[1]

[1]Department of Pediatrics, Kyoto University Graduate School of Medicine, Kyoto, Japan; [2]Clinical Application Department, Center for iPS Cell Research and Application, Institute for Integrated Cell-Material Sciences, Kyoto University, Kyoto, Japan; [3]Division of Pediatrics, Department of Reproductive and Developmental Medicine, Faculty of Medicine, University of Miyazaki, Miyazaki, Japan; [4]Department of Pediatrics, Faculty of Medicine, Osaka University, Suita, Japan; [5]Department of Pediatrics, Osaka Medical College, Takatsuki, Japan; [6]Department of Pediatrics, Hirosaki University Graduate School of Medicine, Hirosaki, Japan; [7]Department of Pediatrics, Kishiwada City Hospital, Kishiwada, Japan; [8]Department of Human Genetics, National Center for Child Health and Development, Tokyo, Japan; [9]Department of Pediatrics, Niigata University, Niigata, Japan; and [10]Department of Pediatrics, Hiroshima University Graduate School of Biomedical Sciences, Hiroshima, Japan

Somatic mosaicism has been described in several primary immunodeficiency diseases and causes modified phenotypes in affected patients. X-linked anhidrotic ectodermal dysplasia with immunodeficiency (XL-EDA-ID) is caused by hypomorphic mutations in the *NF-κB essential modulator (NEMO)* gene and manifests clinically in various ways. We have previously reported a case of XL-EDA-ID with somatic mosaicism caused by a duplication mutation of the *NEMO* gene, but the frequency of somatic mosaicism of *NEMO* and its clinical impact on XL-EDA-ID is not fully understood. In this study, somatic mosaicism of *NEMO* was evaluated in XL-EDA-ID patients in Japan. Cells expressing wild-type NEMO, most of which were derived from the T-cell lineage, were detected in 9 of 10 XL-EDA-ID patients. These data indicate that the frequency of somatic mosaicism of *NEMO* is high in XL-ED-ID patients and that the presence of somatic mosaicism of *NEMO* could have an impact on the diagnosis and treatment of XL-ED-ID patients. (*Blood*. 2012;119(23):5458-5466)

Introduction

X-linked anhidrotic ectodermal dysplasia with immunodeficiency (XL-EDA-ID) is a disease with clinical features including hypohidrosis, delayed eruption of teeth, coarse hair, and immunodeficiency associated with frequent bacterial infections.[1-5] The gene responsible for XL-EDA-ID has been identified as *NF-κB essential modulator (NEMO)*.[6-8] NEMO is necessary for the function of IκB kinase, which phosphorylates and degrades IκB to activate NF-κB.[9-10] Defects in NEMO cause various abnormalities in signal transduction pathways involving NF-κB, and affect factors such as the IL-1 family protein receptors, the TLRs, VEGFR-3, receptor activator of nuclear factor κB (RANK), the ectodysplasin-A receptor, CD40, and the TNF receptor I.[7] Whereas a complete loss of NEMO function in humans is believed to cause embryonic lethality,[11] *NEMO* mutations in XL-EDA-ID patients are hypomorphic,[8] causing a partial loss of NEMO functions.

In XL-EDA-ID, NEMO defects lead to diverse immunologic features including susceptibility to pathogens, impaired Ab response to polysaccharides,[2,4,12] hypogammaglobulinemia,[13] hyper IgM syndrome,[14] and impaired NK-cell activity,[15] with a large degree of variability in phenotypes among the patients. For example, approximately one-tenth of XL-EDA-ID patients exhibit reduced mitogen-induced proliferation of T lymphocytes.[12] Moreover, one-fourth suffer from inflammatory disorders such as inflammatory bowel disease and rheumatoid arthritis,[12] although the inflammatory process usually relies on NF-κB activation.[16] One explanation for this clinical variability is that the XL-EDA-ID phenotype is *NEMO* genotype-specific. Although the XL-EDA-ID database reported by Hanson et al succeeds to some extent in linking the specific clinical features to *NEMO* genotype,[12] the penetrance of some clinical features is not high and the mechanism accounting for this variability is unknown.

Recently, we have reported a case of spontaneous reversion mosaicism of the *NEMO* gene in XL-EDA-ID, which showed an atypical phenotype involving decreased mitogen-induced T-cell proliferation along with decreased CD4 T cells (patient 1).[17] There have been no subsequent reports on somatic mosaicism in XL-EDA-ID, and its prevalence and impact on the clinical features of the disease is unknown. In this study, we describe the younger brother of patient 1, who suffered from XL-EDA-ID with the same mutation and somatic reversion mosaicism of *NEMO*. Patient 2 showed intriguing laboratory findings in that mitogen-induced T-cell proliferation varied in accordance with the rate of detected reversion in the peripheral blood. These 2 cases led us to perform a nationwide study of XL-EDA-ID patients in Japan that revealed a high incidence of somatic mosaicism of *NEMO*.

Submitted May 11, 2011; accepted April 8, 2012. Prepublished online as *Blood* First Edition paper, April 19, 2012; DOI 10.1182/blood-2011-05-354167.

The online version of this article contains a data supplement.

The publication costs of this article were defrayed in part by page charge payment. Therefore, and solely to indicate this fact, this article is hereby marked "advertisement" in accordance with 18 USC section 1734.

Table 1. Clinical and genetic features of XL-EDA-ID patients

Patient	Mutation	Ectodermal dysplasia	Mitogen-induced proliferation	Infections	Complications	Therapy	Sex chromosome chimerism
1	Duplication	+	Reduced	Sepsis (S.P. and P.A.)	Chronic diarrhea	IVIG	100% XY
				Disseminated M.A.C.	Failure to thrive	RFP, CAM, AMK, EB	
				Skin abscess (S.A.)	Small intestinal stenosis	Rifabutin	
				Invasive *Aspergillus*	Lymphedema		
2	Duplication	+	Reduced	Sepsis (*E coli*)	Failure to thrive	IVIG, ST, EB, CAM	99.8% XY 0.2% X
				Disseminated M.S.		Rifabutin, SCT	
3	D311E	−	Normal	Disseminated B.C.G.		IVIG, INH	100% XY
				Sepsis (S.P.)		RFP, SCT	
4	A169P	+	Normal	Meningitis (S.P.)	IBD	IVIG, ST, PSL	99% XY
					Interstitial pneumonia	CyA, MTX, Infliximab	
					Rheumatoid arthritis		
5	L227P	+	Normal	Recurrent pneumonia	IBD	ST, mesalazine	Not done
				Pyogenic coxitis		Infliximab	
				Recurrent otitis media			
6	R182P	+	Not done	Recurrent otitis media	IBD	ST, mesalazine	99.8% XY 0.2% X
				UTI, Recurrent stomatitis			
				Subepidermal abscess			
7	R175P	+	Normal	Recurrent sepsis (S.P.)		IVIG	100% XY
8	Q348X	+	Normal	Disseminated B.C.G.	IBD	IVIG, ST	100% XY
9	R175P	+	Normal	Recurrent pneumonia	IBD	IVIG	100% XY
				Recurrent otitis media		5-aminosalicylic acid	
				Kaposi varicelliform eruption			
10	1167 ins C	+	Normal	Sepsis and Enteritis (E.A)	Failure to thrive	IVIG, SCT	Not done
				Sepsis (C.G.)	Pyloric stenosis, colon polyps		
				UTI (K.P.)			

S.P. indicates *Streptococcus pneumoniae*; P.A., *Pseudomonas aeruginosa*; IVIG, intravascular immunoglobulin infusion; M.A.C., *Mycobacterium avium* complex; S.A., *Staphylococcus aureus*; *E coli*, *Escherichia coli*; ST, trimethoprim-sulfamethoxazole; M.S., *Mycobacterium szulgai*; AMK, amikacin; EB, ethambutol; CAM, clarithromycin; SCT, stem cell transplantation; B.C.G., Bacille de Calmette et Guerin; INH, isoniazid; RFP, rifampicin; IBD, inflammatory bowel disease; PSL, prednisolone; CyA, cyclosporine A; MTX, methotrexate; UTI, urinary tract infection; E.A., *Enterobacter aerogenes*; C.G., *Candida glabrata*; and K.P., *Klebsiella* pneumonia.

Methods

Informed consent

Informed consent was obtained from the patients and their families following the Declaration of Helsinki according to the protocol of the Internal Review Board of Kyoto University, which approved this study.

Patients

Patient 1 was an XL-EDA-ID patient with a duplication mutation of the *NEMO* gene spanning intron 3 to exon 6. This patient has been reported previously[17] and died from an *Aspergillus* infection at the age of 4. Patient 2, born at term, was the younger brother of patient 1. This patient was also diagnosed as XL-EDA-ID with the same duplication mutation as patient 1 by genetic study. He received trimethoprim-sulfamethoxazole prophylaxis and a monthly infusion of immunoglobulin from the age of 1 month. The patient maintained good health and had a body weight of 7899*g* at 6 months when he started to fail to thrive. Except for poor weight gain, patient 2 appeared active with a good appetite, negative C-reactive protein, normal white blood cell counts, and no apparent symptoms. At 19 months of age, *Mycobacterium szulgai* was detected by venous blood culture, and the patient was treated with multidrug regimens including ethambutol, rifabutin, and clarithromycin based on the treatment of systemic *Mycobacterium avium* complex infection. The patient responded well to the treatment and his weight increased from 7830*g* to 9165*g* within a month after the treatment was initiated. Patient 2 received an unrelated cord blood cell transplantation at 26 months of age, containing 8.5×10^7 nucleated cells/kg (4.4×10^5 $CD34^+$ cells/kg), which was matched at 5 of 8 loci: mismatches occurred at 1 HLA-B and 1 HLA-C allele (according to serology), and at 1 HLA-A, 1 HLA-B, and 1 HLA-C allele (according to DNA typing). The preconditioning regimen consisted of fludarabine (30 mg/m^2/d) on days −7 to −3, melphalan (70 mg/m^2/d) on days −6 to −5, and rabbit anti-thymocyte globulin (2.5 mg/kg/d) on days −6 to −2. At first, Tacrolimus (0.024 mg/kg/d) was used to prevent GVHD, but this was switched to cyclosporin A (3 mg/kg/d) on day 9 because of drug-induced encephalopathy. Neutrophil ($> 0.5 \times 10^9$/L) and platelet ($> 50 \times 10^9$/L) engraftment were examined on days 13 and 40, respectively. Although $CD19^+$ cells (2042/μL, 94% donor chimerism), $CD56^+$ cells (242/μL, 97% donor chimerism), and monocytes (557/μL, 69% donor chimerism) were successfully generated, $CD3^+$ cells were not detected in the peripheral blood by day 54. The patient suffered from septic shock and died on day 60. Patients 3 to 10 were XL-EDA-ID patients recruited nationwide in Japan. Clinical details of patients 3, 4, and 10 have been reported previously.[18-20] These patients had clinical phenotypes characteristic of XL-EDA-ID such as ectodermal dysplasia, innate and/or acquired immunity defects, and susceptibility to pyogenic bacteria and *Mycobacterium* infection. Every patient had a mutation in the *NEMO* gene that caused reduced NF-κB activation in a NEMO reconstitution assay, as described in "Proliferation of $NEMO^{normal}$ and $NEMO^{low}$ T cells." Patient profiles are listed in Table 1.

Flow cytometric analysis

NEMO intracellular staining was performed as previously described.[17] The cells were stained for the following lineage markers before staining for NEMO: CD4, CD8, CD14, CD15, CD19, CD56, CD45RA (BD Biosciences/BD Pharmingen), and CCR7 (R&D Systems Inc). Intracellular staining of human IFN-γ, TNF-α, and NEMO was performed as previously described.[18] The stained cells were collected using a FACSCalibur flow cytometer (BD Biosciences) and analyzed using the FlowJo software (TreeStar).

Reporter assay

Wild-type and mutant *NEMO* cDNAs were generated from a healthy volunteer and the recruited XL-EDA-ID patients by RT-PCR; the cDNAs were subcloned into the p3xFLAG-CMV14 vector (Sigma-Aldrich). NEMO null rat fibroblast cells (kindly provided by Dr S. Yamaoka, Department of Molecular Virology, Graduate School of Medicine, Tokyo Medical and Dental University, Tokyo, Japan) were plated at a density of

3×10^4 cells/well in a 24-well culture dish and were transfected with 40 ng of NF-κB reporter plasmid (pNF-κB-Luc; BD Biosciences/BD Clontech), 2 ng of *NEMO* mutant expression construct, 10 ng of internal control for the normalization of transfection efficiency (pRL-TK; Toyo Ink), and 148 ng of mock vector using FuGENE HD Transfection Reagent (TOYO-B-Net) according to the manufacturer's protocol. Twelve hours after transfection, the cells were stimulated with 15 ng/mL lipopolysaccharide (LPS; Sigma-Aldrich) for 4 hours and the NF-κB activity was measured using the PicaGene Dual SeaPansy assay kit (TOYO-B-Net). Experiments were performed in triplicate and firefly luciferase activity was normalized to *Renilla* luciferase activity.

Subcloning analysis of cDNA

Cell sorting of the various cell lineages was performed by FACSVantage (BD Biosciences). The purity of each lineage was > 95%. The cDNA from sorted cells was purified and reverse transcribed by Super Script III (Invitrogen) with random hexamers and amplified by the proofreading PCR enzyme KOD, as previously described.[17,21] The PCR primers used were NEMO2 (5′-AGAGACGAAGGAGCACAAAGCTGCCTTGAG-3′) and NEMO3 (5′-ACTGCAGGGACAATGGTGGGTGCATCTGTC-3′). The PCR products were subcloned using a TA cloning kit (Invitrogen) and sequenced by ABI 3130xl Genetic analyzer (Applied Biosystems). To determine whether additional mutations occurred in revertant subclones that had wild-type sequence in the original mutation site, the entire coding region of the *NEMO* gene was sequenced and an additional mutation was considered present when the same mutation was detected in multiple subclones.

Allele-specific PCR

The mRNA purified from sorted T cells and monocytes was reverse-transcribed by SuperScript III (Invitrogen) with the gene-specific primer NEMO2 and amplified by the proofreading PCR enzyme KOD (Toyobo) using the primers NEMO3 and NEMO 4 (5′-TGTGGACACGCAGT-GAAACGTGGTCTGGAG-3′). The PCR products were used as templates for allele-specific PCRs with Ex Taq polymerase (Takara Bio). Mutant and wild-type *NEMO* DNA was generated from each NEMO expression plasmid, mixed at graded ratios, and used as controls. PCR conditions and primer sequences are listed in supplemental Table 1 (available on the *Blood* Web site; see the Supplemental Materials link at the top of the online article).

Proliferation of NEMO^{normal} and NEMO^{low} T cells

To obtain PHA-induced T-cell blasts, PBMCs were stimulated with PHA (1:100; Invitrogen) and cultured in RPMI 1640 supplemented with 5% FCS and recombinant human IL-2 (50 IU/mL; kindly provided by Takeda Pharmaceutical Company) at 37°C for 7 days. Subcloning analysis of the cDNA obtained from the T-cell blasts was performed as described in "Subcloning analysis of cDNA."

Results

Reversion mosaicism of NEMO occurred in siblings with similar immunologic phenotypes

We previously reported patient 1 with a duplication mutation of the *NEMO* gene spanning intron 3 to exon 6, who was diagnosed as XL-EDA-ID at 1 year of age after suffering from recurrent infections.[17] At first, genetic diagnosis of the patient was difficult because the expression of aberrant *NEMO* mRNA was masked by the expression of normal *NEMO* mRNA by the revertant cells. Flow cytometric analysis of intracellular NEMO expression revealed cells with normal (NEMO^{normal}) and reduced (NEMO^{low}) levels of NEMO expression, indicating the presence of reversion mosaicism of the *NEMO* gene, and further analysis revealed that the *NEMO* mutation was disease-causing. PCR across the mutated region and sequencing of the PCR products revealed a duplication extending from intron 3 to exon 6, which was confirmed by Southern blot analysis. Additional copy number analysis of the *NEMO* gene of patient 1 and his mother excluded the possibility of a complex chromosomal aberration such as multiple duplication of the *NEMO* gene (supplemental Figure 1). Furthermore, polymorphism analysis using variable number tandem repeats on NEMO^{normal} and NEMO^{low} cells from patient 1 revealed that these cells were derived from the same origin (supplemental Table 2), indicating that the *NEMO* gene mosaicism was less likely because of amalgamation. The genomic analysis of the NEMO^{normal} cells revealed a complete reversion of the *NEMO* gene with no additional mutations. The clinical phenotype of patient 1 was combined immunodeficiency with a reduced number of T cells and mitogen-induced proliferation (Tables 2-3). We previously determined that reduced NEMO expression in the mutant T cells caused impairment of T-cell development and mitogen-induced proliferation.

Patient 2, the younger brother of patient 1, was diagnosed as XL-EDA-ID with the same duplication mutation as his brother. Flow cytometric analysis of intracellular NEMO expression performed at diagnosis showed that most of his PBMCs had reduced NEMO expression (Figure 1A). At 2 months of age, when most of the T cells were NEMO^{low}, absolute counts of the patient's T cells and the mitogen-induced proliferation of the patient's PBMCs were comparable with those of the healthy controls (Figure 1A-B; Table 2). These findings indicated that the *NEMO* mutation had no effect on T-cell development and mitogen-induced proliferation during early infancy in patient 2.

NEMO^{normal} T cells gradually increased as patient 2 grew older, while the absolute count of NEMO^{low} T cells decreased (Figure 1A-B). Accordingly, normal full-length *NEMO* cDNA, which had been undetectable in cord blood, was detectable in the patient's peripheral blood at 12 months of age. However, while NEMO^{normal} T cells were increasing, mitogen-induced T-cell proliferation started to decrease (Table 3), and the patient started to show poor weight gain from 6 months of age. When patient 2 was 17 months old, a blood culture revealed an *M szulgai* bacteremia. At this time, the absolute count of NEMO^{normal} T cells peaked, and NEMO^{low} T cells were at a minimum. He began to gain weight after anti-*Mycobacterium* medication was initiated, although NEMO^{normal} T cells started to decrease and NEMO^{low} T cells began to increase (Figure 1B). When the patient was 23 months old, mitogen-induced T-cell proliferation was still low and a roughly equal number of NEMO^{low} and NEMO^{normal} T cells were detected (Table 3). Overall, as patient 2 grew older, NEMO^{normal} T cells increased as the total number of T cells and the mitogen-induced T-cell proliferation decreased, similar to what had occurred in patient 1 at a similar age.

Various analyses were performed to compare the immunologic phenotype of NEMO^{low} and NEMO^{normal} T cells in detail. Both NEMO^{normal} and NEMO^{low} CD4$^+$ T cells carried a diverse Vβ repertoire, but CD8$^+$ T cells had a skewed Vβ repertoire regardless of NEMO expression level (Figure 1C). Surface marker analysis revealed that most of the NEMO^{normal} T cells were CD45RA$^-$/CCR7$^-$ and most of the NEMO^{low} T cells were CD45RA$^+$/CCR7$^-$ (Figure 1D). The NEMO^{normal} T cells produced similar amounts of IFN-γ and TNF-α as healthy control cells, while the production of these cytokines were reduced in NEMO^{low} T cells (Figure 1E-F). Taken together, these data implied that the immunologic phenotype of T cells from patient 2 converged with that of patient 1 as patient 2 grew older.

Table 2. Surface marker analysis of peripheral mononuclear cells of patients 1 and 2

	Patient 1	Patient 2		Healthy controls
Age at analysis	2 y	2 mo	19 mo	
CD3	1503	2366	1014	2997 ± 1751
CD4	292	1583	374	1683 ± 874
CD8	1160	783	547	1114 ± 976
TCRαβ	1386	2295	439	2620 ± 1612
TCRγδ	109	74	574	343 ± 177
$CD4^+CD45RA$	58	1336	105	1471 ± 890
$CD4^+CD45RO$	263	307	266	497 ± 189
$CD8^+CD45RA$	1178	783	297	1083 ± 1078
$CD8^+CD45RO$	361	21	250	385 ± 442
$CD4^+CD25$	80	427	93	210 ± 99
CD19	1200	941	1543	1252 ± 1145
CD20	1189	931	1536	1125 ± 837
$CD19^+$Sm-IgG	7	18	17	54 ± 21
$CD19^+$Sm-IgA	15	4	14	18 ± 14
$CD19^+$Sm-IgM	1171	910	1505	1057 ± 881
$CD19^+$Sm-IgD	1171	906	1495	1052 ± 884
CD16	912	176	24	287 ± 200
CD56	908	176	24	306 ± 207

Surface markers expressed by XL-EDA-ID patients' PBMCs are shown as absolute counts per microliter of peripheral blood. Healthy control values are based on children aged 1 to 6 years and are shown as the mean ± SD.

Sm indicates the surface membrane.

High incidence of somatic mosaicism of the *NEMO* gene in XL-EDA-ID patients

It is worth noting that somatic reversion mosaicism of the *NEMO* gene occurred in both of the 2 XL-EDA-ID siblings carrying a duplication mutation. To determine whether a high frequency of reversion is a specific event for this type of *NEMO* duplication mutation[22-25] or if the reversion of the *NEMO* gene occurs commonly in XL-EDA-ID patients, we recruited an additional 8 XL-EDA-ID patients from throughout Japan (Table 1) and analyzed the presence of *NEMO* reversion. These patients had various combinations of clinical phenotypes characteristic of XL-EDA-ID such as ectodermal dysplasia, innate and acquired immunity defects, and susceptibility to pyogenic bacteria and *Mycobacterium* infections. Every patient had a mutation of the *NEMO* gene with reduced NF-κB activation potential, as evaluated in a NEMO reconstitution assay (Figure 2).

Among the 8 patients, only patient 3 had a large proportion of $NEMO^{low}$ cells by flow cytometric analysis. The majority of patient 3's PBMCs were $NEMO^{low}$, whereas 10% of the patient's $CD8^+$ cells were $NEMO^{normal}$ (Figure 3A). This patient was identified as carrying the D311E mutation. Because missense mutations of the *NEMO* gene often do not result in the reduced expression of NEMO protein, subcloning and sequencing analysis was performed on the *NEMO* cDNA isolated from the remaining patients, and 6 of the 7 patients had normal *NEMO* subclones (Table 3). Expansion of maternal cells after fetomaternal transfusion was ruled out in these patients by FISH analysis with X and Y probes (Table 1).

Additional genetic analysis of the entire coding region of the *NEMO* gene was performed on $NEMO^{normal}$ cells from patient 3 and on reverted subclones from the other patients, except for patient 10 who had already received stem cell transplantation. The *NEMO* gene in these samples had reverted to wild-type with no additional mutations (Figure 3B and data not shown). To specifically determine in which cell lineages the reversion occurred, subcloning and sequencing analysis of cDNA in various cell lineages was performed. This analysis revealed that all the revertant cells were of the T-cell lineage and that no reversion occurred in monocytes and very little occurred in B cells (Table 4). Allele-specific PCR confirmed that reversion occurred in T cells but not in monocytes (Figure 4).

Selective advantage of $NEMO^{normal}$ cells in XL-EDA-ID carriers

The high frequency of somatic mosaicism in T cells of XL-EDA-ID patients indicated a strong selective advantage of wild-type NEMO T cells over T cells carrying mutant NEMO. To confirm this hypothesis, *NEMO* cDNA analysis was performed on various cell lineages from the mothers of the patients who are heterozygous for *NEMO* mutation and thus have mosaicism

Table 3. Immunologic analysis of patients 1 and 2

	Patient 1	Patient 2 (treated with IVIG)	
Age at analysis, mo	9	9	20
Serum immunoglobulin levels, g/L (control)			
IgG	10.63 (4.51-10.46)	8.44 (4.51-10.46)	10.37 (7.15-9.07)
IgA	1.36 (0.14-0.64)	1.88 (0.14-0.64)	3.93 (0.22-1.44)
IgM	0.4 (0.33-1.00)	0.17 (0.33-1.00)	0.20 (0.34-1.28)
Age at analysis	2 y	2 mo	23 mo
T-cell proliferation, SI (control)	9.3 (206.9 ± 142.5)	55.3 (64.8 ± 8.1)	7.2 (89.4 ± 31.2)

Control values of serum immunoglobulin levels are based on children aged either 7 to 9 months or 1 to 2 years and are shown as the mean ± SD. The T-cell proliferation assay was performed as described previously[17] with at least three healthy adults as controls.

SI indicates stimulation index; and IVIG, 2.5 g of monthly IV immune globulin infusion.

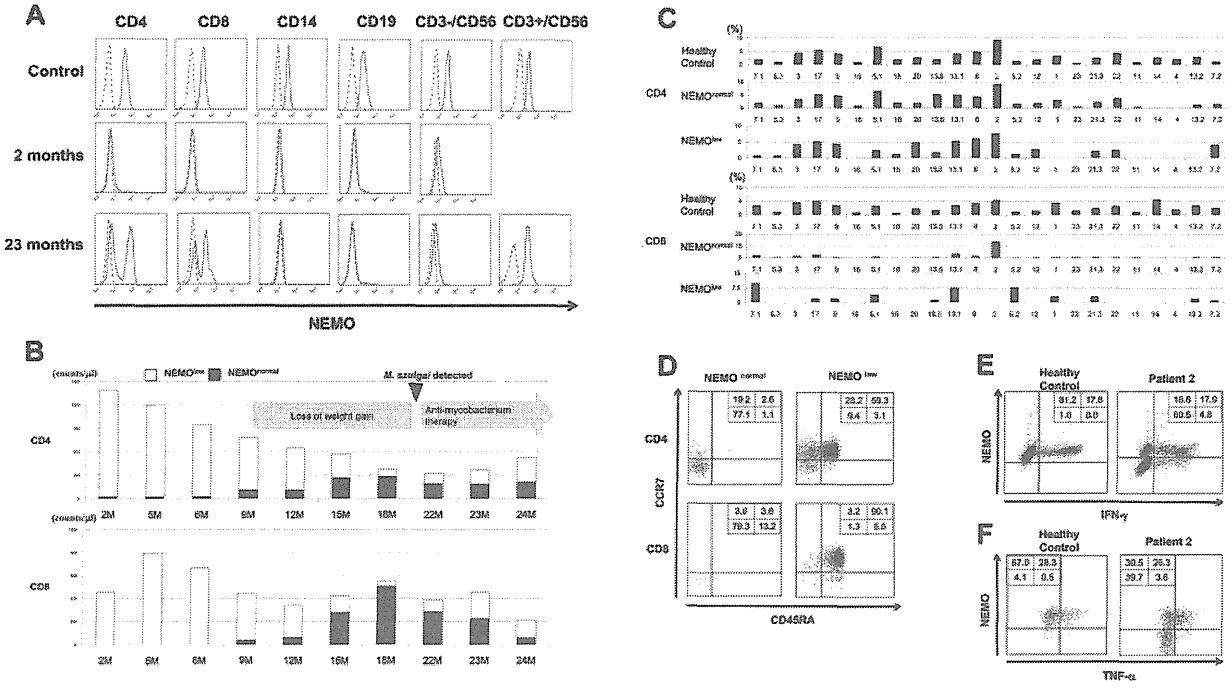

Figure 1. Identification and characterization of *NEMO* revertant T cells in patient 2. (A) Intracellular expression of NEMO in various PBMC lineages from a healthy adult control and patient 2 were evaluated by flow cytometry. For the patient, results of the analyses performed at 2 months and 23 months are shown. Solid lines indicate staining with the anti-NEMO mAb, and dotted lines indicate the isotype control. (B) Time-course variations in the absolute count of $NEMO^{normal}$ and $NEMO^{low}$ T cells in patient 2. M indicates age in months. (C) TCR-Vβ repertoire analysis of the patient's $CD4^+$ and $CD8^+$ T cells. PBMCs from the patient and a healthy adult control were stained for the TCR-Vβ panel, CD4, CD8, and NEMO, and analyzed by flow cytometry. (D) Phenotype analysis of T cells in patient 2. PBMCs from the patient and a control were stained for the expression of NEMO, CCR7, CD45RA, and CD4 or CD8. Data shown were gated on $NEMO^{normal}$ or $NEMO^{low}$ $CD4^-$ or $CD8^+$ cells. (E-F) Cytokine production from $NEMO^{normal}$ and $NEMO^{low}$ T cells. PBMCs from the patient and a control were stimulated with PMA and ionomycin for 6 hours and stained for intracellular (E) IFN-γ or (F) TNF-α along with NEMO. Cells shown are gated on the $CD3^+$ population.

because of X-chromosome inactivation. This analysis assumes that the percentage of cDNA for wild-type *NEMO* reflects the percentage of cells expressing wild-type NEMO. A high proportion of wild-type *NEMO* cDNA was observed in T cells from the mothers of patients 1/2, 3, 8, and 10, although wild-type *NEMO* cDNA was not predominant in T cells from the mother of patient 4 (Table 5).

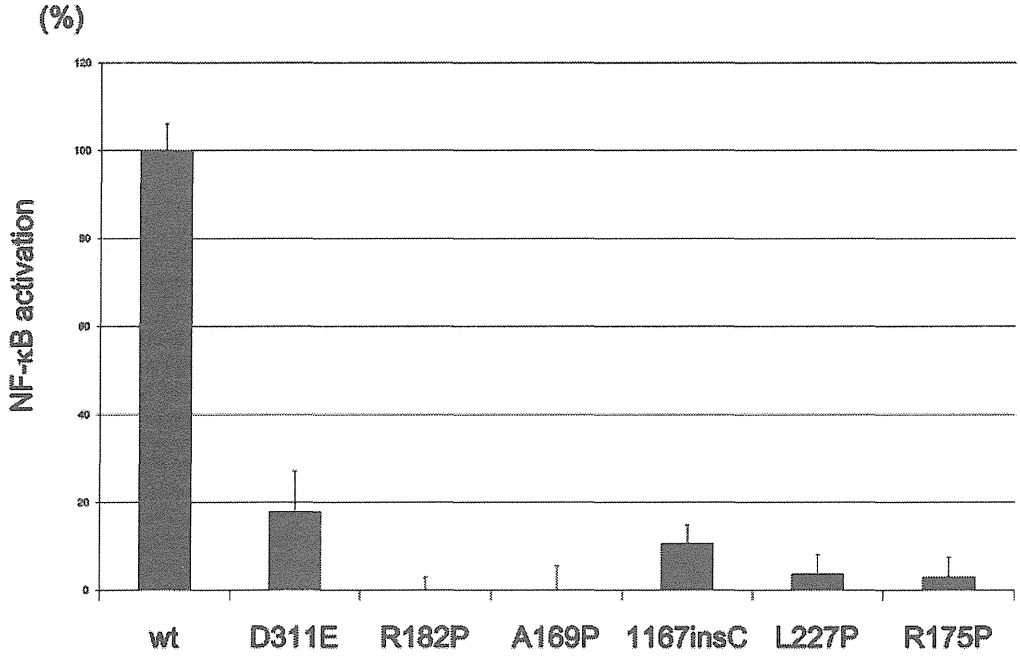

Figure 2. NF-κB transactivation by NEMO mutants from the XL-EDA-ID patients. NF-κB transactivation induced by NEMO mutants in the XL-EDA-ID patients. Mock vectors and wild-type (wt) NEMO were used as controls. The NF-κB activation index of NEMO variants were calculated as (NF-κB activation by each NEMO variant − NF-κB activation of the mock vector)/(NF-κB activation by wild-type NEMO − NF-κB activation of the mock vector). The data shown are the mean ± SD of triplicate wells and are representative of 3 independent experiments with similar results.